Document downloaded from:

http://hdl.handle.net/10251/195287

This paper must be cited as:

Noguerol-Meseguer, AT.; Igual Ramo, M.; Pagán Moreno, MJ. (2022). Developing psyllium fibre gel-based foods: Physicochemical, nutritional, optical and mechanical properties. Food Hydrocolloids. 122:1-12. https://doi.org/10.1016/j.foodhyd.2021.107108

The final publication is available at

https://doi.org/10.1016/j.foodhyd.2021.107108

Copyright Elsevier

Additional Information

OBJETIVE

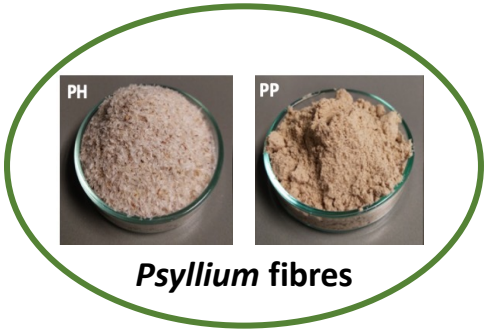

***Psyllium* fibres**

characterization

METHODOLOGY

Characterization

- Hydration properties
- Physicochemical properties
- Phenols content
  Antioxidant capacity
  Mineral content

Gel formation

Back extrusion

- Rheology
- TPA

Physicochemical properties

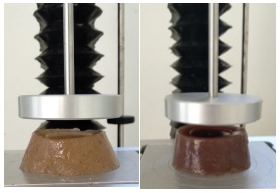

PH PP

RESULTS

Characterization

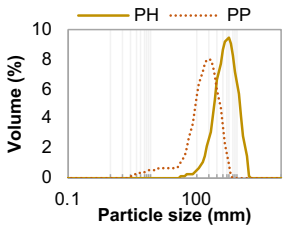

PP ↑ Phenols content
Antioxidant capacity

PH ↑ Hydration properties

Gel formation

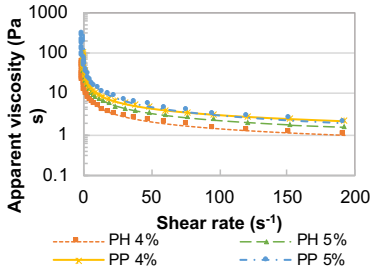

PH & PP → Gelling properties → 5 °C / 65 °C

Avoid negative effects on food

New textures and new products

Developing *Psyllium* fibre gel-based foods: physicochemical, nutritional, optical and mechanical properties

Ana Teresa Noguerol, Marta Igual, Mª Jesús Pagán*

Universitat Politècnica de València, Food Technology Department, Food Investigation and Innovation Group, Camino de Vera s/n, 46022, Valencia, Spain

**Corresponding author. E-mail address: jpagan@tal.upv.es (M. J. Pagán).*

Abstract

Psyllium fibre has known health benefits, which are highly related to its gelling properties, so it is important to know the functional properties and its gelling capacity to its possible incorporation as a new source of DF in foods. Therefore, the purpose of this research was to evaluate these properties of two *Psyllium* fibres. Physicochemical (particle size distribution, pH, water content, water activity, hygroscopicity and bulk density and porosity), hydration (water holding, water retention and swelling capacity, fat absorption capacity and solubility), and nutritional properties (mineral content, total phenolics compounds and antioxidant capacity) of dietary fibre (DF) samples were recorded. Moreover, physicochemical (water content, pH and colour) and mechanical properties (back extrusion test, rheological measurement and texture profile analysis) of gel samples were performed before and after heat treatment (20 min at 65 °C). The hydration properties of Plantago Husk (PH) were higher than those in Plantago Powder (PP), but in functional terms, high values of phenols and antioxidant activity were found in PP. However, both samples displayed similar gelling properties. As a result of the rheological and textural analysis, both fibres showed good gelling properties at both high (65 °C) and cool (5 °C) temperatures, at concentrations 4% to 7%. Moreover, the results indicate

28 that PH and PP have suitable characteristics to be functional ingredients, which can help
29 to avoid possible negative effects on food sensory and structural characteristics.
30
31 **Keywords:** *Psyllium* fibre; hydration properties; functional capacity; gelling properties.
32

1. INTRODUCTION

There is a growing awareness about diet and health, which has brought about changes in consumer eating habits and the demand for healthier foods has increased (de Moraes Crizel, Jablonski, de Oliveira Rios, Rech, & Flôres, 2013). Fibre was one of the first ingredients to be associated with health in the 1980s and has been used by the food industry ever since (Dervisoglu, & Yazici, 2006; de Moraes Crizel et al., 2013). Plants high in dietary fibre (DF) and natural antioxidants have drawn increasing attention in recent years (Zhu, Huang, Peng, Qian, & Zhou, 2010). DF consumption offers several health benefits, including body weight control, reduced serum lipid and cholesterol, controlled postprandial glucose responses and colon cancer prevention, which are attributed to the physicochemical and functional properties of DF (Ma, & Mu, 2016). DFs also have well-known technological functions, such as water absorption and water retention and can, thus, reduce shrinkage, cooking loss and drip loss during storage, and can minimise production costs without affecting final products' sensory properties (Han, & Bertram, 2017). Thus the emergence of new fibre sources and processing methods to improve fibre's functionality has extended its applications in the food industry. Further, they have opened new possibilities to design new fibre-enriched products and generate new textures for a variety of applications (Rosell, Santos, & Collar, 2009).

Psyllium seed husk (*Plantago ovata*) is a source of natural DF that is of interest for food and pharmaceutical sciences as a functional ingredient (Ren, Linter, & Foster, 2020a). It comprises arabinoxylan, a polymer rich in arabinose and xylose, whose digestibility in humans is limited (Jalanka et al., 2019). *Psyllium* has been used in traditional medicine worldwide (Fradinho, Soares, Niccolai, Sousa, & Raymundo, 2020; Ren, Yakubov, Linter, MacNaughtan, & Foster, 2020b). Ren et al. (2020b) and Franco, Sanches-Silva, Ribeiro-Santos, and Ramos de Melo (2020) have reported that *Psyllium* husk seed has good water absorbability with gelling properties, and can be used as a hydrocolloid for functional applications in food production. Hydrogels in food are mostly applied for structuring purposes to gain desirable rheological or textural properties, and for

stabilising foams, dispersions, emulsions and particles. In recent years, hydrogels have drawn attention for their applications to deliver food bioactives (Mao, Lu, Cui, Miao, & Gao, 2020). Much research has been conducted into *Psyllium* health benefits for diabetes, constipation, colon cancer prevention, diarrhoea, inflammatory bowel disease (ulcerative colitis), irritable bowel syndrome symptoms, abdominal pain, obesity and hypercholesterolaemia (Guillon & Champ, 2000; Jane, McKay, & Pal, 2019; Franco et al., 2020; Belorio, Marcondes, & Gómez, 2020, Ren et al., 2020b). It also contributes to satiety, hypocholesterolaemia and prebiotics (Jalanka et al., 2019; Fradinho et al., 2020; Franco et al., 2020).

It is important to point out that the purpose of this research was to carry out a simpler and more practical characterisation of different commercial *Psyllium* than those found in the literature (Fischer et al., 2004; Yin et al., 2012; Benaoun et al., 2017; Patel, Tanna, Mishra & Jha, 2018; Patel et al., 2019) to facilitate the choice and its possible application by companies in the development of new products and modification of existing ones.

In order to determine *Psyllium* fibre applications, it is vital to characterise and evaluate them according to their functional properties. So this study aimed to characterise two commercial *Psyllium* fibres to know their physicochemical properties, phenol content, antioxidant properties and mineral contents, and to characterise the physicochemical, textural and rheological gels that form to elucidate their potential use in food products. This characterisation could help to avoid possible negative effects on food sensory and structural characteristics, and also to provide new textures to develop new foods.

2. MATERIAL AND METHODS

2.1. Samples

Two *P. ovata* samples were herein used: Plantago Powder (PP) and Plantago Husk (PH). All these samples were supplied by Productos Pilarica S.A. (Paterna, Spain). The names, ingredients and proximate composition of the samples are shown in Table 1 and Fig. 1.

89

90 **2.2. *Psyllium* samples analysis**

91 All the *Psyllium* samples were analysed in triplicate for each analysis.

92

93 **2.2.1. Particle size distribution**

94 Sample particle size distribution was determined by applying the laser diffraction method
95 and Mie theory following the ISO13320 regulation (AENOR 2009) in a particle size
96 analyser (Malvern Instruments Ltd., Mastersizer 2000, UK) equipped with a dry sample
97 dispersion unit (Malvern Instruments Ltd., Scirocco 2000). The volume (in percent)
98 against particle size (in micrometres) was obtained and the size distribution was
99 characterised by the volume mean diameter (D[4,3]). The standard percentiles d(0.1),
100 d(0.5), and d(0.9) represent the particle size below which 10%, 50% and 90% of the
101 sample lies, respectively. These parameters were estimated by the Mastersizer 2000
102 software (version 5.6) considering the particle diameter.

103

104 **2.2.2. Water content and water activity**

105 Water content (x_w) (g water/100 g sample) was determined by vacuum oven drying
106 (Vaciotem, J.P. Selecta, Spain) at 70 °C until constant weight (AOAC, 2000). Samples'
107 water activity (a_w) was analysed by the AquaLab PRE LabFerrer equipment (Pullman,
108 USA).

109

110 **2.2.3. pH**

111 Samples' pH was measured upon dispersions (10% w/v) of samples in distilled water
112 following described methods (Bender et al., 2020).

113

114 **2.2.4. Hygroscopicity**

115 Samples (about 0.2 g in a Petri dish) were placed at 25 °C in an airtight plastic container
116 with Na_2SO_4 saturated solution (81% RH). After 1, 5, and 7 days, each sample was

weighed and hygroscopicity (Hg) was expressed as g of water gained per 100 g dry solids (Cai & Corke, 2000).

2.2.5. Bulk density and porosity

The porosity (ε), or percentage of air volume related to the total volume, was calculated from the true (ρ) and bulk (ρ_b) densities using $\varepsilon = (\rho-\rho_b) / \rho$ according to Igual, García-Segovia and Martínez-Monzó (2021). Samples' real density was determined by a helium pycnometer (AccPyc 1330, Micromeritics, Norcross, USA). For the bulk density (ρ_b) determination, about 2 g of the powder were placed inside a 10 mL graduated test tube and the occupied volume was noted. Bulk density was calculated by dividing the powder mass by occupied volume, expressed as g/L.

2.2.6. Determination of hydration properties

Water-holding capacity (WHC) and water retention capacity (WRC) were determined as described by Raghavendra, Rastogi, Raghavarao, and Tharanathan (2004) and by Chantaro, Devahastin, and Chiewchan (2007). WHC and WRC were determined by placing 1 g of sample in a calibrated cylinder and then adding 30 mL of distilled water. Samples were hydrated for 18 h at 25 °C. WRC tubes were centrifuged at 3,000 ×*g* for 20 min. Finally for both determinations, supernatants were removed, and the hydrated residues were weighed and dried at 100 °C for 3 h until constant weight. The results were expressed as g water/g dry sample.

Swelling water capacity (SWC) was determined as described by Navarro-González, García-Valverde, García-Alonso, & Periago (2011) with slight modifications. One gram of sample was placed in a graduated test tube and hydrated with 20 mL of distilled water. The sample was stored for 18 h at 25 °C, and then the bed volume was recorded. SWC was expressed as volume mL/g sample.

The water solubility index (WSI) was established by the method of Mahdavi, Jafari, Assadpour, and Ghorbani, (2016) with slight modifications. Samples (approx. 1 g) were

145 mixed in centrifuge tubes with 30 mL of distilled water for 5 min until mixtures became
146 homogeneous. Solutions were then incubated at 37 °C in a water bath for 30 min.
147 Afterwards, tubes were centrifuged at 17,640 ×*g* for 20 min at 4 °C. Supernatants were
148 collected and dried in an oven at 100 °C until constant weight. The results were
149 expressed as a percentage.
150 Following the method reported by Navarro-González et al. (2011) with minor
151 modifications, fat adsorption capacity (FAC) was determined. Samples (4 g) were placed
152 in a centrifuge tube with 24 g of sunflower oil. Contents were stirred for 30 sec every 5
153 min for 30 min. Later samples were centrifuged at 1,600 ×*g* for 25 min. Free oil was
154 decanted and FAC was expressed as g oil/g sample.
155
156 **2.2.7. Ash and mineral content**
157 The method 930.05 of AOAC procedures (Horwith, & Latimer, 2005) was used to
158 determine the total ash content. A sample (500 mg) was incinerated at high pressure in
159 a microwave oven (Muffle P Selecta Mod.367PE) for 24 h at 550 °C, and ash was
160 gravimetrically quantified.
161 The multimineral determination was made in an inductively coupled plasma optical
162 emission spectrometer, model 700 Series ICP-OES of Agilent Technologies (Santa
163 Clara, USA), with axial viewing and a charge coupled device detector as described in
164 García-Segovia, Igual, Noguerol, and Martínez-Monzo (2020). Mineral compositions
165 (macro- and microelements) were expressed as mg/100 g sample.
166
167 **2.2.8. Total phenolic compounds**
168 The extraction of total phenols (TP) comprised homogenising a sample with methanol
169 and HCL (6N), and then centrifuging according to Tomás-Barberán, et al. (2001). TP
170 were quantified by the method of Selvendran, and Ryden (1990) and Benzie, and Strain
171 (1999) based on the Folin-Ciocalteu method. Absorbance was measured at 765 nm in a
172 UV-visible spectrophotometer (Thermo Electron Corporation, USA). Total phenolic

content was expressed as mg of gallic acid equivalents (GAE) (Sigma-Aldrich, Germany) per 100 grams of sample using a standard curve 0-800 mg range of gallic acid /mL.

2.2.9. Antioxidant capacity

Antioxidant capacity (AC) was assessed using the free radical scavenging activity of the samples evaluated with stable radical 1,1-diphenyl-2-picrylhydrazyl (DPPH) (Sánchez-Moreno et al., 2003) following the methodology of Igual et al. (2016). A UV-visible spectrophotometer (Thermo Electron Corporation, USA) was used to measure absorbance at 515 nm. The percentage of DPPH was calculated in the same way as other authors (Igual et al., 2019). The final results were expressed as milligram Trolox equivalents (TE) per 100 grams of sample (mg TE/100 g) using a Trolox calibration curve within the 10-500 mg/L range (Sigma-Aldrich, Germany).

2.3. Preparation of gels

In order to prepare the gel samples, fibre powders were dissolved in cold water (5 °C) for 30 min at the 1, 2, 3, 4, 5, 6 and 7% concentrations. Then samples were divided into two batches. One of them was directly stored under cold conditions (24 h at 5 °C) until gel stabilisation. However, the other batch was subjected to heat treatment at 65 °C for 20 min before being stored at 5 °C for 24 h. After storing them, samples were tempered at 25 °C before carrying out the analysis.

2.4. Gel analysis

2.4.1. Water content and pH

Water content (x_w) (g water/100 g sample) was performed as in the powder fibres.

The gel samples' pH determined with a pH-meter Crison MultiMeter MM 41 (Hach Lange, Spain).

2.4.2. Colour

In order to determine gel colour, the CIE*L*a*b* colours were measured according to García-Segovia et al. (2020) with a Konica Minolta CM-700d colorimeter (Konica Minolta CM-700d/600d series, Tokyo, Japan). Measurements were taken on white and black backgrounds by taking D65 as a standard light and 10° as a standard observer. In order to determine samples' translucency, the Kubelka–Munk theory for multiple scattering to the reflection spectra was applied (Talens, Martinez-Navarrete, Fito, & Chiralt, 2002). The calculated reflectance of an infinitely thick layer of a material was used to obtain samples' coordinate CIE*L*a*b* parameters that presented translucency.

2.4.3. Back extrusion test

A back extrusion test was performed according to the method described by Cevoli et al. (2013) with minor modifications. Textural characteristics were evaluated at all the sample concentrations (1-7%) by a TA-XT2 Texture Analyser (Stable Micro Systems Ltd, Godalming, UK) equipped with an extrusion disc (25.4 mm in diameter) positioned centrally over the sample plastic container (diameter: 50 mm, height: 75 mm) with 40 g of sample (approximately 30 mm height). The test was performed at a depth of 50% at the 1 mm/s test speed. The attributes calculated from the force-deformation curve were consistency (N s) (area under the curve up), firmness (N) (maximum force), cohesiveness (N) (maximum negative force) and viscosity (N s) (resistance to flow off the disc).

2.4.4. Rheological measurements

Flow curves were performed only at the 4, 5, 6, and 7% concentrations, at which the consistency results of the back extrusion test were lower than 100 N s, as measured by a Kinexus pro^{+} rotational rheometer (Malvern Instruments, Worcestershire, UK) and the rSpace software, equipped with a system of coaxial cylinders (C25/PC25). A sample (20 mL) was loaded in the geometry and rested to equilibrate for 3 min to achieve a

228 temperature equilibrium (25 °C) and stress relaxation in a heat-controlled sample stage
229 (Peltier Cylinder Cartridge, Malvern Instruments, Worcestershire, UK). According to the
230 method described by Cevoli et al. (2013) with slight modifications, samples were
231 exposed to a logarithmically increase shear rate from 0 to 200 s^{-1} in 3 min. Flow curves
232 were evaluated using the *Ostwald -de Waele* (Eq. (1)) rheological model, where σ is the
233 shear stress (Pa), γ is the shear rate (s^{-1}), *k* is the consistency coefficient (Pa s^n) and *n*
234 the flow behaviour index (dimensionless).This model is used to describe flows of
235 rheologically complex fluids (Shapovalov, 2017). The apparent viscosity at the 50 s^{-1}
236 shear rate (η_{ap}) were calculated (Ribes, Peña, Fuentes, Talens, & Barat, 2020). Each
237 flow curve was performed in triplicate at each sample concentration.
238
239 $$\sigma = k\,\gamma^n \qquad \text{Eq. (1)}$$
240
241 **2.4.5. Texture profile analysis (TPA)**
242 The texture profile analysis (TPA) was performed only on the sample concentrations
243 from 4% to 7%, which presented consistency over 100 N s. Forty grams of each gel
244 preparation concentration were weighed inside a cylindrical plastic container (diameter:
245 50 mm, height: 75 mm). Gel structures were removed from the container before the
246 analysis, which was performed by a TA-XT2 Texture Analyser (Stable Micro Systems
247 Ltd, Godalming, UK) and the Texture Exponent software (version 6.1.12.0). Following
248 the method described by Ağar et al. (2016), a double compression cycle test was run up
249 to 50% strain compression of the original portion height using an aluminium cylinder
250 probe (diameter: 75 mm).
251
252 **2.5. Statistical analysis**
253 An analysis of variance (ANOVA), with a confidence 95% level ($p < 0.05$), by the
254 Statgraphics Centurion XVII Software, version 17.2.04, was applied to evaluate

differences in samples. A correlation analysis of all the studied parameters with a 95% significance level was carried out (Statgraphics Centurion XVII).

3. RESULTS AND DISCUSSION

3.1. Psyllium fibres analysis

3.1.1. Physicochemical properties

Particle size distribution is an important parameter that determines fibre functionality and role in the digestive tract (transit time, fermentation, and faecal excretion) (Rosell, Santos, & Collar, 2009). Fig. 2 shows the particle size distribution in all the samples; as we can see, these samples vastly differed. PH presented the highest particle size, between 40 and 1,660 μm, but with a narrow range of particles between 40 and 105 μm. The particle size for PP was lower, and was distributed from 3 to 631 μm, and concentrated mostly between 40–631 μm. Table 2 shows the volume mean diameter (D[4,3]) and the standard percentiles d(0.1), d(0.5), and d(0.9) of samples' particle size. These differences in the samples' particle size distribution implied that the differences in D[4,3], d(0.1), d(0.5) and d(0.9) were significant ($p < 0.05$).

Table 2 shows the physicochemical properties (a_w, x_w, pH, and Hg); significant differences in a_w and x_w were found between samples ($p < 0.05$). According to the a_w values of by the tested samples, PP presented the lowest a_w, which are similar to those found by de Moraes Crizel et al. (2013). According to Fernández-López et al. (2009), the ideal a_w to avoid microorganism growth and degradation reactions in products with a low water content is between 0.11 and 0.40. Both our tested samples fell within this range. PH showed the highest x_w, with a value of 5.93 (0.14) g_w/100 g sample. These values are like some commercial DF of the different sources found by Rosell, Santos, and Collar (2009), but were lower than those shown by Chong, Ball, McRae, and Packer (2019) for *Psyllium* husk (10.53 g/100 g). The samples' pH values were similar, but significant differences were seen between them ($p < 0.05$). PP had a significantly higher pH than PH ($p < 0.05$). The hygroscopicity (Hg) of PH was significantly higher than PP ($p < 0.05$).

283 In storage terms, lower hygroscopicity could be more positive given the importance of its
284 flowability factor (Moghbeli, Jafari, Maghsoudlou, & Dehnad, 2020).
285 The bulk density (ρ_b) and porosity (ε) of the samples are presented in Table 2. The
286 samples with a lower ρ_b had a higher ε, and *vice versa*. In addition, small, but significant
287 differences were found for these parameters ($p < 0.05$). The sample with the lowest ρ_b
288 was PH. Lan et al. (2012) reported lower ρ_b values for *Polygonatum odoratum*, but they
289 were similar to cellulose (0.38 g/mL). In addition, there were significant Pearson
290 correlations among ρ_b with D[3,4], d(0.1), d(0.5), and d(0.9) ($p < 0.05$) being -0.9888, -
291 0.9855, -0.9876, and -0.9905, respectively. Therefore, the lower D[4,3], d(0.1), d(0.5),
292 and d(0.9) the higher ρ_b because a fibre with a low bulk density should show more
293 surface area and polar groups, which could make both its swelling capacity and oil-
294 binding capacity increase (Lan et al., 2012; Tejada-Ortigoza, Garcia-Amezquita, Serna-
295 Saldívar, & Welti-Chanes, 2016). Uronic acid was detected in polysaccharides extracted
296 from leaves or seeds of *Psyllium* (Zhang et al., 2019), this acid together with the polar
297 groups and a more surface area to the surrounding water leads to an increase in the
298 swelling volume (Tejada-Ortigoza et al., 2016).
299
300 **3.1.2. Mineral content**
301 Table 3 shows the ash content, total minerals and individual mineral content of both
302 samples (Figs. S1 and S2 original equipment graphs). For both ash and total mineral
303 contents, significant differences were found between PP and PH ($p < 0.05$), where PP
304 had the highest ash and mineral contents, which could be associated because the PP
305 sample came from seed (Table 1). Regarding the individual mineral content, no
306 significant differences ($p > 0.05$) were observed between both DF samples (PP and PH)
307 in Se, Zn and Cu contents. For the other analysed minerals, significant differences ($p <$
308 0.05) were present between the PP and PH DF samples, and the P, K, Ca, Na, Fe and
309 Mn values were higher for PP. The results of Ca, Fe and Cu in *Plantago psyllium* and
310 *Plantago ovata* obtained by Ziemichód, Wójcik and Różyło (2019) were comparable to

311 those presented for the PH sample. In addition, Bukhsh, Malik, and Ahmad (2007)
312 showed similar results in *Psyllium* seed husk to K, Ca and Mn found in the PH sample.
313 Chong et al. (2019) obtained similar values to the PH sample for both ash content and
314 Ca, Mg, and Fe minerals in *Psyllium* husk. However, the Fe value for the PP sample,
315 and also for other trace elements like Mn, Zn and Cu of both samples, should be
316 highlighted because, as Rousseau et al. (2020) pointed out, Fe and Zn deficiency poses
317 global health problems with about 30-33% of the world's population at risk, predominantly
318 in underdeveloped countries.
319
320 **3.1.3. Total phenolic compounds and antioxidant capacity**
321 Table 3 shows the studied samples' TP content and antioxidant capacity (AC). The PP
322 TP and AC values were significantly higher than for the other sample ($p < 0.05$). This
323 was probably due to this sample coming from seed compared to PH, which came from
324 *Psyllium* husk. The TP and AC values obtained for PH were like those presented by
325 Chong et al. (2019) for *Psyllium* husk. However, the TP content for PP was higher than
326 that found by Navarro-González et al. (2011) for tomato peel fibre. According to our
327 results, the TP content of the *Psyllium* samples was positively and significant compared
328 to the studied samples' AC ($p < 0.05$). The Pearson correlation between TP and AC was
329 0.9458. Thus, TP strongly affected AC, which coincides with other authors for Lulo
330 (*Solanum quitoense*) (Igual et al., 2014) and grapefruit (Igual et al., 2019). Given the high
331 TP content of PP, we highlight the remarkable attributes and quality as an alternative
332 source of DF. The TP content presented positive correlations with ash, total mineral
333 content, P, K, Ca, Na, Mg, Fe and Mn (0.9693, 0.9782, 0.9633, 0.9927, 0.9645, 0.9178,
334 0.9260, 0.9347 and 0.9474, respectively) ($p < 0.05$), and also with AC (0.8944, 0.9701,
335 0.9815, 0.9563, 0.9434, 0.9135, 0.9637, 0.9671 and 0.9972, respectively). However, this
336 could be negative as DF and components like polyphenols are related to lower mineral
337 absorption in the small intestine due to binding and/or physical entrapment.
338 Nevertheless, this is believed to be balanced for DF fermentation in the colon by gut

339 microflora as the short-chain fatty acids that form can release trapped minerals to
340 increase the absorptive surface area and their absorption, which is significant in the
341 event of deficiency (Baye, Guyot, & Mouquet-Rivier, 2017).
342
343 **3.1.4. Hydration properties**
344 The hydration properties of DF are related to the chemical structure of component
345 polysaccharides, and other factors porosity, particle size, ionic forms, pH, temperature,
346 ionic strength, type of ions in solution and stresses on fibres (Elleuch et al., 2011). These
347 properties partly determine the fate of DF in the digestive tract and account for some of
348 their physiological effects (Guillon, & Champ, 2000). The definition of WHC is the amount
349 of water retained by a sample without being subjected to stress (Rosell, Santos, & Collar,
350 2009). PH and PP showed significant differences for WHC ($p < 0.05$) (Table 2), and PH
351 had the highest and PP the lowest WHC values. The WHC values of these DF were
352 higher than the values found by Rosell, Santos, and Collar (2009) for all the tested
353 commercial fibres, except for inulin (11.05 g/g), and those observed by Kwinda, Onipe,
354 and Jideani (2018) (3.83 g/g) for *Psyllium* fibre, but were markedly lower than those
355 reported by Chong et al., (2019) (45 g/g) for *Psyllium* husk fibre. As in the results by Zhu
356 et al. (2010) revealed for wheat bran DF before and after grinding, WHC increases with
357 a larger particle size because a reduction in particle size may alter the fibre matrix
358 structure.
359 WRC has DF's ability to retain water when subjected to an external force, such as
360 centrifugation (Ma, & Mu, 2016). Table 2 shows the WRC values of the tested samples
361 and the significant differences appeared between PH and PP ($p < 0.05$). These results
362 were notably lower than those of Kale, Yadav, and Hanah (2016) (45.7 g/g), but were
363 higher than those reported by Kwinda, Onipe, and Jideani (2018) (4 g/g) for *Psyllium*
364 fibre. The WRC of PH was higher than the value of Lan et al. (2012) for the DF isolated
365 from *P. odoratum* by being left to dry in the sun (23.94 g/g), but the PP value was lower
366 than that for cellulose (12.42 g/g). According to de Moraes Crizel et al. (2013) and

Grigelmo-Miguel and Martin-Belloso (1999), DF with high WRC values can be used as a functional food ingredient to reduce calories, avoid syneresis and modify both the viscosity and texture of processed food. SWC is the volume occupied by a known fibre weight under the employed condition. In addition, SWC and WRC provide not only an overview of fibre hydration, but also useful information for fibre-supplemented foods (Guillon, & Champ, 2000). The SWC of PH was significantly higher than that of PP ($p < 0.05$) (Table 2). Guillion, and Champ (2000) reported a list of fibres' hydration properties with different particle sizes where the range of SWC values was from 5.5 to 11.9 mL/g. Accordingly, the SWC values of both the tested samples fell within this range.

The nature of the glycidyl component and the structural characteristics of fibre are involved in the WSI, which is expressed as the percentage of the fraction that is solubilised under defined conditions (de Moraes Crizel et al., 2013). PP had higher solubility, and significant ($p < 0.05$) differences appeared between samples (Table 2). The high solubility of PP could be due to it being a sample with a high soluble fibre (SDF) (data from suppliers in Table 1). It is also well-known that high solubility can inhibit the digestion and absorption of nutrients from the gut (Guillon, & Champ, 2000), such as glucose and cholesterol (Belorio, Marcondes, & Gómez, 2020). Besides, soluble fibres have shown a better ability to provide viscosity and to form gels or act as emulsifiers (Elleuch et al., 2011). The WSI results for PP was higher than those reported by de Moraes Crizel et al. (2013) for DF from orange (28.95%), but lower than shown by Femenia et al. (1997) for DF from cauliflower florets dried at 75 °C (48.1%). However, the WSI value was lower for PH.

FAC is fibre's ability to absorb fat or oil, which is important in nutrition for preventing fat loss while cooking because fat is absorbed in the intestinal lumen, which lowers cholesterol (Navarro-González et al., 2011; Ma, & Mu, 2016) and retains food flavours (de Moraes Crizel et al., 2013). Table 2 shows the FAC of the tested samples. The FAC of PH was higher than that of PP, and significant differences were found between samples ($p < 0.05$). The PH value was higher than the values shown for fibre from tomato

395 peel (1.46 g oil/g) by Navarro-González et al. (2011), and was similar to that found by
396 Femenia et al. (1997) for cauliflower stem fibre dried at 40 °C (2.1 g oil/g). However, the
397 PP value was similar for the tomato peel fibre value indicated by Navarro-González et
398 al. (2011).
399 The ability of *Psyllium* of absorb water and oil is by the interaction between the hydroxyl
400 groups of water and those of the polysaccharide macromolecules present in the mucilage
401 (Chaplin, 2003; Dikeman and Fahey, 2006; Beikzadeh et al., 2017). Polysaccharides
402 obtained from seeds and husk of *Psyllium* are comprised of xylose, galactose, rhamnose,
403 arabinose (Patel et al., 2019); then, molecules such as arabinose and xylose create the
404 hydrogen bonds in the mucilage (Beikzadeh et al., 2017). The hydrophilic feature of
405 mucilage causes interaction between water and increases water retention capacity
406 during cooking and storage (Beikzadeh et al., 2017).
407 The physicochemical parameters and hydration properties are related, a correlation
408 analysis between parameters was conducted (Table 4). All the hydration properties
409 showed statistically significant Pearson's correlation coefficients when related to D[4,3],
410 d(0.1), d(0.5), d(0.9), Hg and pH ($p < 0.05$). Hygroscopicity showed positive correlations
411 with hydration properties, except for the WSI, where higher Hg led to a better ability to
412 absorb water and oil. Moreover, a_w and x_w correlated positively with WHC, WRC and
413 FAC, but negative correlations with the WSI, and no correlations with SWC were found.
414 However, pH correlated positively with WHC and the WSI, but negatively with SWC,
415 WRC and FAC. Bulk density (ρ_b) correlated negatively with WHC, WRC and FAC, but
416 positively with the WSI. When ρ_b had high values, the capacity of DF to bind water and
417 oil decreased, but high ρ_b values meant increased DF solubility. However, particle size
418 (D[4,3], d(0.1), d(0.5), d(0.9)) was positively related to hydration properties, except for
419 the WSI. When samples' particle size grew, the absorption capacity of water and oil
420 increased, but samples' solubility decreased. It can be generally stated that a reduced
421 particle size is related to a diminished ability to retain water and oil (Lan, Chen, Chen, &

422 Tian, 2012), but this effect cannot be generalised because both the chemical structure
423 and shape of DF also play an essential role (Rosell, Santos, & Collar, 2009). Besides,
424 authors like Zhu et al. (2010), Lan et al. (2012), and Ma, and Mu (2016) supported this
425 correlation by reporting similar results. Conversely, other authors like Chantaro et al.
426 (2008) and Rosell et al. (2009) showed that for a smaller particle size, fibres were better
427 able to bind water. These authors also showed the importance of not generalising and
428 analysing each fibre type because, as Tejada-Ortigoza et al. (2016) stated, these
429 properties are related to environmental conditions, the chemical structure of the DF
430 polysaccharides, and to treatments and/or extraction conditions.
431 Moreover, a correlation analysis between the multimineral content and hydration
432 properties was performed (Table 4). The total mineral content showed statistically
433 significant negative Pearson's correlation coefficients when related to all the hydration
434 properties (SWC, WHC, WRC and FAC), except for the WSI, which had a positive
435 correlation ($p < 0.05$). Additionally, minerals P, K, Ca, Na, Mg, Fe and Mn correlated
436 negatively with WHC, WRC and FAC, but positively with the WSI. This situation could be
437 related to the valence and ratio of the adsorbed ions, because the ion valence increased
438 or the ratio decreased, and the hydration force magnitude increased (Li et al., 2020). For
439 this reason, these minerals must be divalent ions because they are adsorbed in
440 completely hydrated states (Li et al., 2020). However, SWC was negatively associated
441 with K and Ca.
442
443 **3.2. Gel analysis**
444 **3.2.1. Physicochemical and optical properties**
445 Solutions of both DF samples were prepared at the 1, 2, 3, 4, 5, 6, and 7% concentrations
446 (heated and unheated) to know the physicochemical and mechanical properties of each
447 concentration, and their possible different uses in food. Table 5 shows both samples' x_w,
448 pH and solution colour at each concentration. The x_w of both samples lowered when the
449 DF concentration rose in both (with and without heat treatment). An interaction occurred

between samples' concentration and the employed DF sample (PP or PH) when x_w lowered as the concentration of both DF samples increased. With PP, the drop in the 6% and 7% concentrations was significantly more marked ($p < 0.05$) regardless of the temperature at which structures formed.

The pH of the tested gels was similar for both samples, and the pH went from 6 to 7. However, significant differences were observed in the pH values of both samples with and without heat treatment ($p < 0.05$) (Table 5). An interaction between concentration and used DF sample (PP of PH) was observed, and the pH values slight dropped for both DF samples when concentration rose ($p < 0.05$). For pH, the most marked decrease was observed in the PH sample up to the 3% fibre concentration (with and without heat treatment). The sample with the highest pH was 65PH at the 1% concentration. No significant effect on the pH values was observed in the solution concentrations for the PH fibre because of heat treatment ($p > 0.05$), whereas the solutions made with the PP fibre had slightly lower pH values in the heated samples ($p < 0.05$).

With both samples, when the DF samples' concentration went below 4%, the solid content precipitated. When the concentration rose, dispersion homogeneity markedly increased because samples were mixtures of whole cells and dispersed cell wall materials of different particle sizes, as shown in Fig. 2. Therefore, the bigger material absorbed water until it formed a stabler gel structure. Table 5 depicts the colorimetric parameters (L*, a* and b*) of the formulated samples. To illustrate the colour samples, the images of gels are presented in Fig. 3 (with and without heat treatment). It can be seen that, although both samples came from *Psyllium*, gel colours significantly differed ($p < 0.05$), which could be due to the fact that PP came from *Plantago ovata* seed and PH came mostly from husk (Table 1). Similar behaviour was observed in the gels made with both samples, and parameters L*, a* and b* significantly increased with a rising fibre concentration both with and without heat treatment ($p < 0.05$). As observed in this study, Wang et al. (2018) reported that the colour parameters increased in the homogenised suspension and became more saturated with red and yellow. The colour of gel samples

478 depended mainly on the colour of solids as seen in Fig. 1, where PP was markedly
479 darker. The increase observed in the colour parameters was also related to the used DF,
480 and the PP gels generally had higher L* and a* values in the unheated and heated
481 samples ($p < 0.05$), but lower b* values. Moreover, no significant differences were
482 observed in either luminosity (L*) or redness (a*) for the DF sample (PP or PH) and the
483 applied treatment ($p > 0.05$). Both samples displayed the same behaviour, but
484 yellowness (b*) significantly decreased, which was observed when samples were
485 prepared with heat treatment in the gels formulated with PP ($p < 0.05$). The colour of
486 these samples was darker than the gels made with hydrocolloids like xanthan gum
487 (Chong et al., 2019). Other authors have indicated that the incorporating *Psyllium* into
488 different food products can increase colour darkness in products (Ahmadi, Kalbasi-
489 Ashtari, Oromiehie, Yarmand, & Jahandideh, 2012; Figueroa, & Genovese, 2019). Gel
490 colour is related to mineral content because positive Pearson correlations were found.
491 The increase in the luminosity (L*) of both samples (heated and unheated) can be
492 associated with a higher total mineral content (0.8699), and Ca and Na showed a higher
493 correlation (0.8898 and 0.8877, respectively). However, an increase in redness (a*) was
494 more related to the total mineral content when samples were heated (0.8507.; Na, Ca,
495 Mg, K, P and Fe were the minerals that were the most related to a rise in a* when gels
496 were formed with heat (0.8233, 0.8218, 0.8128, 0.8115, 0.8062 and 0.8022,
497 respectively). For yellowness (b*), a higher and positive correlation was also found with
498 the total mineral content when gels formed without heat treatment (0.8463). In this case,
499 K, P, Fe, Mg and Mn were the minerals that most strongly influenced the increase in b*
500 (0.8976, 0.8923, 0.8874, 0.8801 and 0.8559, respectively).
501
502 **3.2.2. Mechanical properties**
503 The back extrusion assay was performed at all the gel concentrations (1-7%), similarly
504 to a previous study in order to know the mechanical properties of both *Psyllium* DFs (Fig.
505 S3 original graphs). Table 6 depicts the back extrusion parameter results. This table

506 indicates that not only the consistency and firmness of *Psyllium* gels increased as the
507 DF concentration rose, but so did viscosity and cohesiveness as results showed by
508 Noguerol, Igual and Pagán-Moreno (2021) for different DFs. However, the results of this
509 study showed that both *Psyllium* fibres had greater values of all back extrusion
510 parameters than DFs showed by Noguerol, Igual and Pagán-Moreno (2021). Moreover,
511 a significant interaction took place between concentration and temperature ($p < 0.05$),
512 and all the back extrusion parameters increased when the gels were heated. This
513 increase in consistency was similar in the gels with both the *Psyllium* DF samples. The
514 gelling process begins with the formation of junction zones, these junctions grow and
515 join the polysaccharide molecules to form the gel network (Yu, Perret, Parker, & Allen,
516 2003).However, the interaction between treatment and the employed DF sample was
517 observed for firmness, cohesiveness and viscosity where the gels formulated with the
518 PP sample obtained significantly higher results for these parameters from the 5%
519 concentration ($p < 0.05$), except for viscosity, which presented significant differences
520 only in the 7% concentration. It is a well-known fact that *Psyllium* fibre has positive gelling
521 properties (Yu et al., 2003) and Askari et al. (2018) indicated that the gels formulated
522 with *Psyllium*-maize starch films had a more compact and homogeneous structure than
523 the films made only with starch. Therefore as this study indicates, both *Psyllium* fibres
524 can be used as gelling agents in food products with or without starch addition. In line with
525 the result shown in this study, Ren et al. (2020b) indicated that hydrated whole *Psyllium*
526 husk powder exhibited a gel-like property and this gel became stronger when it was
527 formed by applying heating. Authors like Igual et al 2013 and Igual et al., 2014 indicated
528 that some parameters like consistency and viscosity are very important because they
529 are related to coverage in mouth with gelled products.
530 The Pearson correlations indicated that all the back extrusion parameters (consistency,
531 firmness, viscosity, cohesiveness) were associated with samples' x_w, pH, and mineral
532 composition. A negative correlation between x_w and pH with consistency (-0.8044 and -
533 0.7445, respectively) and firmness (-0.7777 and -0.7141) was found, and a positive

correlation appeared between x_w and pH with viscosity (0.9035 and 0.8081, respectively) and cohesiveness (0.8923 and 0.7992, respectively). The total mineral content was positively related to consistency and firmness (0.7494 and 0.7636, respectively), and Ca (0.8267 for consistency and 0.8176 for firmness) and Na (0.8247 for consistency and 0.8154 for firmness) were the most influential minerals. However, viscosity and cohesivity negatively correlated with total mineral content (-0.8149 and -0.8609, respectively). In this case, Ca (-0.8939 for viscosity and -0.9213 for cohesiveness) and Na (-0.8859 for viscosity and -0.9223 for cohesiveness) were the most influential minerals. In practice, Li et al. (2018) and Liu et al. (2018) indicated that the gelation of food biopolymers could be induced by different approaches, including temperature, pressure, acids, salts, enzymes, ethanol, among others. From the results of this study, the consistency and firmness of the *Psyllium* gels increased with a lower pH. It can also be stated that gel formation is due to ionic interactions with Ca and Na (Mao et al., 2020). The consistency, firmness and viscosity parameters of the gels formed at cold temperature (5 °C) were also associated with DF samples' SWC, and negatively with firmness and consistency (-0.8740 and -0.8698, respectively) and positively with viscosity (0.8886). However, consistency was positively related to the WSI (0.8143). When gels were formed with heating, a negative Pearson correlation with WHC was found (-0.8187).

As the 1%, 2% and 3% concentrations were not homogeneous and did not form a stable hydrogel, a decision was made to perform flow curves and TPA from only concentrations 4% to 7%. Hence the samples with a consistency lower than 100 N s as a result of the back extrusion assay were characterised by the flow curve analysis (Fig. S4 original graphs). Consistency (*k*), flow behaviour (*n*) and goodness of fit (R^2) are shown in Table 7. All the data were fitted with Ostwald's power law. The PP gels had the highest *k* and an increase in *k* was related to a rising DF concentration, Su, Zhu, Adhikari, Li, and Wang (2020) indicated the same results for the citrus fibre-oil dispersions. On the contrary, no significant differences were observed between the gels made with PH fibre ($p > 0.05$).

All the formulated gels had a *k* higher than 20 Pa s. So their gelling properties can be identified with semisolid or spoonable foods (Aguayo-Mendoza et al., 2019), and can be used as fat replacers and/or texture modifiers of meat analogues, among others. *n* was lower than 1 in all the samples, which means that our samples behaved as pseudoplastic fluids. As no changes were observed in *n* due to increasing PH fibre content ($p > 0.05$), the rising PP concentration led to a significant decrease in this parameter ($p < 0.05$).

Both *k* and *n* were related to particle size (D[4,3] and d (0.9)). For *k*, a negative Pearson correlation was presented, which meant that a drop in *k* was associated with a bigger particle size (-0.9211 for D[4,3] and -0.9757 for d (0.9)). However, positive correlations were found between D[4,3] and d (0.9) with *n* (0.8822 and 0.9545, respectively). Wang et al. (2018) have also reported that this parameter depends on particle size distribution.

Pearson correlations were found between the flow curve parameters and hydration properties, except for SWC. *k* and η_{ap} were negatively related to WHC (-0.9427 and -0.8861, respectively), WRC (-0.9939 and -0.8766, respectively) and FAC (-0.9933 and -0.8394, respectively), but positively with the WSI (0.9914 and 0.8123, respectively). *n* was positively correlated with WRC and FAC, and negatively with the WSI (0.8862, 0.9111 and -0.9252, respectively).

Dikeman and Fahey (2006) (p. 652) indicated that *"viscosity as related to DF refers to the ability of some polysaccharides to thicken or form gels when mixed with fluids resulting from physical entanglements among the polysaccharides constituents within the fluid or solution"* and apparent viscosity is the most common term in the literature related to DF. The trend of samples' apparent viscosity is shown in Fig. 4, where it can be observed that the tendency of all the gels was similar, although the PH samples seemed to have lower apparent viscosity. Table 7 confirms this. It shows the samples' η_{ap} and that no concentration dependences were found with either sample ($p > 0.05$), but both the η_{ap} of the PP gels was significantly higher than it was for the PH gels ($p < 0.05$). These results agree with the reports by Agarwal, Hewson, and Foster (2018), and shear viscosity was related to fibres' source, processing and microstructure. Therefore in line

590 with Ren et al. (2020b), freshly prepared *Psyllium* husk dispersion can be described as
591 the concentrated suspension of gel particles and its rheological properties can be
592 ascribed to particles' viscoelastic properties and to the physical contacts and friction
593 between them. It is noteworthy that authors like Niknam, Ghanbarzadeh, Ayaseh, and
594 Rezagholi (2018) have reported that the addition of *Plantago major* seed to emulsions
595 can enhance the stability of samples during storage by increasing continuous phase
596 viscosity. Therefore, this could also be achieved by adding PP and/or PH. The present
597 study confirms both fibres can be used as texturizing agents to modify the food texture
598 to pudding-like consistency (> 1750 mPa s) for patients with oropharyngeal dysphagia
599 (Ribes, Estarriaga, Grau, Talens, 2021).
600 When characterisation ended, a TPA was performed in those samples that presented a
601 higher back extrusion consistency than 100 N s (Fig. S5 original graphs). The TPA
602 parameter results are shown in Table 8. Regarding the hardness results for the gels
603 formed without heat, it can be seen that the different concentrations of each DF sample
604 ($p > 0.05$), but the hardness of the gels formulated with PP was significantly higher ($p <$
605 0.05). When gels were formed by heating, concentration fibre dependence was found for
606 both samples, as was a high DF concentration and marked hardness. This increased
607 hardness was greater for the PH gels than for PP one. The highest results were for the
608 65PH sample at 7% ($p < 0.05$). A heat treatment effect appeared for the PH sample, and
609 the hardness of the gels formed by heating with the DF sample was higher, high
610 temperature fractions have stronger gel properties (Ren et al., 2020b). Comparing these
611 results with gels formed with other vegetable fibres (Noguerol, Igual, Pagán-Moreno,
612 2021), *Psyllium* gels form more stable and firmer gels
613 All the results for adhesiveness were negatives, which indicated that it formed a sticky
614 gel. The PH samples with no heat treatment presented lower adhesiveness than the gels
615 formed at 65 °C, but the adhesiveness for the PP gels decreased when gels were formed
616 with heating. It could be related to the different composition of the *Psyllium* fibre, because
617 the PP fibre is from the seed and has more proteins and carbohydrates (Table 1) which

618 can modify its conformation with heating. In addition, Ren et al. (2020b) indicated that
619 during heating, the gel phase gradually expanded and disappeared, which might play
620 the role of junction zone formation and responsible for the thermoreversible gel-like
621 properties. An interaction was observed between adhesiveness and the increased DF
622 concentration with both samples. The importance of this parameter lies in food texture
623 becoming unpleasant for consumers when it adheres to the palate and requires much
624 effort to separate it. It can be noted that springiness was similar for all the samples and
625 did not depend on the used fibre or concentration. Although, formulations with high
626 adhesiveness caused prolonged retention in buccal cavity (Bhatia & Ahuja, 2013).
627 Regarding cohesiveness, the gel samples with heat treatment generally obtained
628 significantly higher results ($p < 0.05$). It also depended on the DF used because the
629 cohesiveness of PP was greater ($p < 0.05$) at the highest concentration tested in this
630 study.
631 The chewability of both *Psyllium* samples was higher than the gel formed with a
632 combination of bamboo, psyllium and citric fibre presented by Noguerol, Igual and
633 Pagán-Moreno (2021). The highest chewability value was for the 65PH 7% gel. This
634 parameter also depended on fibre concentration for the gels formed at 65 °C. Authors
635 like Fradinho, Soares, Niccolai, Sousa, and Raymundo (2020) have indicated that both
636 hardness and adhesiveness are dependent on the *Psyllium* concentration in pasta, and
637 that pasta with *Psyllium* is less adhesive due to this material's gelling properties, which
638 favour a more cohesive structure with less cooking loss. As in the back extrusion assay,
639 positive correlations were found between hardness and Ca and Na minerals (0.6720 and
640 0.6607, respectively), but a negative correlation was observed when adhesiveness was
641 related to these minerals (-0.7258 and -0.7143, respectively). With the cohesiveness
642 Pearson correlations, this was associated with minerals K and Mn (0.6078 and 0.6056,
643 respectively) but, as with hardness, chewability showed a relation with Ca and Na
644 (0.6893 and 0.6789, respectively). As a result, both fibres PP and PH displayed gelling
645 properties at not only lower temperatures (65 °C), but also at cool temperatures (5 °C).

This should be highlighted because these samples can be used to adapt the texture of different foods, while supplementation with *Psyllium* fibres implies potential health benefits (Jalanka et al., 2019; Jane, McKay, & Pal, 2019). As with back extrusion and flow curves, the TPA parameters were also related to the hydration properties of the DF samples. When samples were formed without heat treatment, hardness correlated negatively with WHC, WRC and FAC (-0.8564, -0.9114 and -0.9069, respectively), and positively with the WSI (0.9247). On the contrary, adhesiveness was positively related to WHC, WRC and FAC (0.9443, 0.9150 and 0.9101, respectively) and negatively to the WSI (-0.8839). The resilience and chewability of the cold gels were associated with all the hydration properties: negatively with WHC, WRC, SWC and FAC and positively with the WSI (respectively -0.8996, -0.8917, -0.9415, -0.9034 and 0.9534 for resilience; -0.9015, -0.9521, -0.7637, -0.9518 and 0.9673 for chewability). However, when gels were formed with heating, relations were noted only between the cohesiveness and hydration properties, with negative correlations with WHC, WRC and FAC (-0.9099, -0.9758 and -0.9714, respectively), and a positive correlation with the WSI (0.9671). Therefore, gel structure formation (heating or not) depended on the hydration properties of the DF samples.

3.3. Practical implications of this study

The clean label trend has emerged due to the concern of consumers about healthiness and sustainability of food products (Euromonitor International, 2016). Moreover, the COVID-19 health crisis has increased the concern for a healthy lifestyle (Academia Española de Nutrición y Dietética, 2020). Thus, the importance to include DF in our diet, since it offers health benefits for body weight control, cholesterol, diabetes, constipation, diarrhoea, inflammatory bowel disease, irritable bowel syndrome symptoms, and colon cancer prevention (Ma, & Mu, 2016; Franco et al., 2020; Belorio, Marcondes, & Gómez, 2020).

673 For these reasons, according to the results obtained in this study, these two *Psyllium*
674 fibres could be used as new clean label texturizers, as well as to avoid the negative
675 effects in foods such as cooking loss, drip loss, syneresis, and fat loss. In addition, they
676 could also be used as fat replacers or to develop new plant-based products, since one
677 of the main problems for their development is texture. Furthermore, one of the main
678 reasons for the lower consumption of plant-based products by omnivores is because
679 they do not like the texture and flavour (Fiestas-Flores & Pyhälä, 2018; Noguerol, Pagán,
680 García-Segovia & Varela, 2021). This DF could also be used to adapt food products to
681 patients with oropharyngeal dysphagia, because one of the most employed strategies to
682 overcome this problem is the use of texturing agents that modifies foods texture (Ribes
683 et al., 2021).
684
685 **4. CONCLUSIONS**
686 This study revealed that PH had the highest values for hydration properties, thus could
687 be a functional ingredient to avoid physical food properties, such as syneresis and fat
688 loss during cooking, and to improve textural and sensory characteristics. However, the
689 AC, the TP and the mineral content for PP were higher, which is a highlighted finding in
690 quality terms as an alternative source of DF. As a result of the rheological and textural
691 analysis, both fibres showed good gelling properties from concentration 4% to 7% at both
692 high (65 °C) and cool (5 °C) temperatures. These properties generally depended on the
693 DF concentration. According to these results, both PH and PP could lead to different gel
694 types that would allow their use as new sources of DF in food with different
695 characteristics, a use that could promote health benefits for human health. In addition,
696 they could also be used as fat replacers, to develop new products, to modified textures
697 and to adapt food products to elderly people. However, further studies in different foods
698 are required to check behaviour with other ingredients and to adjust the suitable
699 concentration to each food type.
700

5. ACKNOWLEDGEMENTS

The authors acknowledge the financial support of the Generalitat Valenciana (programme FDEGENT 2018) and the company Productos Pilarica S.A. (Paterna, Spain).

6. DECLARATION OF INTEREST

The authors declare no conflict of interest.

7. REFERENCES

Academia Española de Nutrición y Dietética Consejo General de Colegios oficiales de Dietistas-Nutricionistas, RED de Nutrición Basada en la Evidencia. (2020). *Recomendaciones de Alimentación y Nutrición Para la Población Española Ante la Crisis Sanitaria del COVID-19*. Madrid. Available online at: https://academianutricionydietetica.org/NOTICIAS/alimentacioncoronavirus.pdf

Ağar, B., Gençcelep, H., Saricaoğlu, F. T., & Turhan, S. (2016). Effect of sugar beet fiber concentrations on rheological properties of meat emulsions and their correlation with texture profile analysis. *Food and Bioproducts Processing, 100*, 118-131.

Agarwal, D., Hewson, L., & Foster, T. J. (2018). A comparison of the sensory and rheological properties of different cellulosic fibres for food. *Food & function, 9*(2), 1144-1151.

Ahmadi, R., Kalbasi-Ashtari, A., Oromiehie, A., Yarmand, M. S., & Jahandideh, F. (2012). Development and characterization of a novel biodegradable edible film obtained from psyllium seed (Plantago ovata Forsk). *Journal of Food Engineering, 109*(4), 745-751.

AOAC. (2000). Official Methods of Analysis. Association of Official Analytical Chemist. *Volume I, agricultural chemicals, contaminants, drugs / edited by William Horwitz.* EUA.

Askari, F., Sadeghi, E., Mohammadi, R., Rouhi, M., Taghizadeh, M., Shirgardoun, M. H., et al. (2018). The physicochemical and structural properties of psyllium gum/ modified starch composite edible film. *Journal of Food Processing and Preservation, 42*(10), e13715.

Baye, K., Guyot, J. P., & Mouquet-Rivier, C. (2017). The unresolved role of dietary fibers on mineral absorption. *Critical Reviews in Food Science and Nutrition, 57*(5), 949-957.

Beikzadeh, S., Peyghambardoust, S., Homayouni, R. A., & Beikzadeh, M. (2017). Effects of psyllium and marve seed mucilages on physical, sensory and staling properties of sponge cake. *Journal of Agricultural Science and Technology, 19*, 1079-1089.

Belorio, M., Marcondes, G., & Gómez, M. (2020). Influence of psyllium versus xanthan gum in starch properties. *Food Hydrocolloids*, 105843.

Benaoun, F., Delattre, C., Boual, Z., Ursu, A. V., Vial, C., Gardarin, C., Wadouachic, A., Le Cerfd, D., Varacavoudind, T., El-Hadj, M. D. O., Michauda, P., & Pierre, G. (2017). Structural characterization and rheological behavior of a heteroxylan extracted from Plantago notata Lagasca (Plantaginaceae) seeds. *Carbohydrate polymers*, *175*, 96-104.

Bender, A. B. B., Speroni, C. S., Moro, K. I. B., Morisso, F. D. P., dos Santos, D. R., da Silva, L. P., & Penna, N. G. (2020). Effects of micronization on dietary fiber composition, physicochemical properties, phenolic compounds, and antioxidant capacity of grape pomace and its dietary fiber concentrate. *LWT, 117,* 108652.

Benzie, I.F.F., & Strain, J.J. (1999). Ferric reducing/antioxidant power assay: direct measure of total antioxidant activity of biological fluids and modified version for simultaneous measurement of total antioxidant power and ascorbic acid concentration. *Methods in Enzymology*, *299*, 15-27.

Bhatia, M., & Ahuja, M. (2013). Thiol modification of psyllium husk mucilage and evaluation of its mucoadhesive applications. *The Scientific World Journal*, 2013.

Bukhsh, E., Malik, S. A., & Ahmad, S. S. (2007). Estimation of nutritional value and trace elements content of Carthamus oxyacantha, Eruca sativa and Plantago ovata. *Pakistan Journal of Botany, 39*(4), 1181.

Cai, Y. Z., & Corke, H. (2000). Production and properties of spray-dried Amaranthus betacyanin pigments. *Journal of food science, 65*(7), 1248-1252.

Cevoli, C., Balestra, F., Ragni, L., & Fabbri, A. (2013). Rheological characterisation of selected food hydrocolloids by traditional and simplified techniques. *Food hydrocolloids, 33*(1), 142-150.

Chantaro, P., Devahastin, S., & Chiewchan, N. (2008). Production of antioxidant high dietary fiber powder from carrot peels. *LWT-Food Science and Technology*, *41*(10), 1987-1994.

Chaplin, M. F. (2003). Fibre and water binding. *Proceedings of the Nutrition Society, 62*(1), 223-227.

782 Chong, R. W. W., Ball, M., McRae, C., & Packer, N. H. (2019). Comparing the chemical
783 composition of dietary fibres prepared from sugarcane, psyllium husk and wheat
784 dextrin. *Food chemistry*, *298*, 125032.
785
786 de Moraes Crizel, T., Jablonski, A., de Oliveira Rios, A., Rech, R., & Flôres, S. H. (2013).
787 Dietary fiber from orange byproducts as a potential fat replacer. *LWT-Food Science and*
788 *Technology, 53*(1), 9-14.
789
790 Dervisoglu, M., & Yazici, F. (2006). Note. The effect of citrus fibre on the physical,
791 chemical and sensory properties of ice cream. *Food Science and Technology*
792 *International*, *12*(2), 159-164.
793
794 Dikeman, C. L., & Fahey Jr, G. C. (2006). Viscosity as related to dietary fiber: a review.
795 *Critical reviews in food science and nutrition, 46*(8), 649-663.
796
797 Elleuch, M., Bedigian, D., Roiseux, O., Besbes, S., Blecker, C., & Attia, H. (2011). Dietary
798 fibre and fibre-rich by-products of food processing: Characterisation, technological
799 functionality and commercial applications: A review. *Food chemistry*, *124*(2), 411-421.
800
801 Euromonitor International (2016). *Report extract: Lifestyle 2016: New survey insights*
802 *and system refresher.*
803
804 Femenia, A., Lefebvre, A. C., Thebaudin, J. Y., Robertson, J. A., & Bourgeois, C. M.
805 (1997). Physical and sensory properties of model foods supplemented with cauliflower
806 fiber. *Journal of food science*, *62*(4), 635-639.
807

808 Fernández-López, J., Sendra-Nadal, E., Navarro, C., Sayas, E., Viuda-Martos, M., &
809 Pérez-Álvarez, J. A. (2009). Storage stability of a high dietary fibre powder from orange
810 by-products. *International journal of food science & technology*, *44*(4), 748-756.
811
812 Fiestas-Flores, J., & Pyhälä, A. (2018). Dietary motivations and challenges among
813 animal rights advocates in Spain. *Society & Animals, 26*(4), 402-425.
814
815 Figueroa, L. E., & Genovese, D. B. (2019). Fruit jellies enriched with dietary fibre:
816 Development and characterization of a novel functional food product. *LWT-Food Science*
817 *and Technology*, 111, 423-428.
818
819 Fischer, M. H., Yu, N., Gray, G. R., Ralph, J., Anderson, L., & Marlett, J. A. (2004). The
820 gel-forming polysaccharide of psyllium husk (Plantago ovata Forsk). *Carbohydrate*
821 *research*, *339*(11), 2009-2017.
822
823 Fradinho, P., Soares, R., Niccolai, A., Sousa, I., & Raymundo, A. (2020). Psyllium husk
824 gel to reinforce structure of gluten-free pasta? *LWT-Food Science and Technology*, *131*,
825 109787.
826
827 Fradinho, P., Soares, R., Niccolai, A., Sousa, I., & Raymundo, A. (2020). Psyllium husk
828 gel to reinforce structure of gluten-free pasta?. *LWT, 131*, 109787.
829
830 Franco, E. A. N., Sanches-Silva, A., Ribeiro-Santos, R., & de Melo, N. R. (2020). Psyllium
831 (Plantago ovata Forsk): From evidence of health benefits to its food application. *Trends*
832 *in Food Science & Technology*, *96*, 166-175.
833

834 García-Segovia, P., Igual, M., Noguerol, A. T., & Martínez-Monzó, J. (2020). Use of
835 insects and pea powder as alternative protein and mineral sources in extruded snacks.
836 *European Food Research and Technology, 246*(4), 703-712.
837
838 Grigelmo-Miguel, N., & Martín-Belloso, O. (1999). Comparison of dietary fibre from by-
839 products of processing fruits and greens and from cereals. *LWT-Food Science and*
840 *Technology*, *32*(8), 503-508.
841
842 Guillon, F., & Champ, M. (2000). Structural and physical properties of dietary fibres, and
843 consequences of processing on human physiology. *Food research international*, *33*(3-
844 4), 233-245.
845
846 Han, M., & Bertram, H. C. (2017). Designing healthier comminuted meat products: Effect
847 of dietary fibers on water distribution and texture of a fat-reduced meat model
848 system. *Meat Science*, *133*, 159-165.
849
850 Horwith, W., & Latimer, G. W. (2005). AOAC International, 18th ed.
851
852 Igual, M., Cebadera, L., Cámara, R. M., Agudelo, C., Martínez-Navarrete, N., & Cámara,
853 M. (2019). Novel Ingredients Based on Grapefruit Freeze-Dried Formulations: Nutritional
854 and Bioactive Value. *Foods*, *8*(10), 506.
855
856 Igual, M., Contreras, C., & Martínez-Navarrete, N. (2014). Colour and rheological
857 properties of non-conventional grapefruit jams: Instrumental and sensory measurement.
858 *LWT-Food Science and Technology, 56*(1), 200-206.
859

Igual, M., García-Martínez, E., Camacho, M. M., & Martínez-Navarrete, N. (2017). Stability of micronutrients and phytochemicals of grapefruit jam as affected by the obtention process. *Food Science and Technology International*, *22*(3), 203-212.

Igual, M., García-Martínez, E., del Mar Camacho, M., & Martínez-Navarrete, N. (2013). Physicochemical and sensorial properties of grapefruit jams as affected by processing. *Food and Bioprocess Technology, 6*(1), 177-185.

Igual, M., García-Segovia, P., & Martínez-Monzó, J. (2021). Resistant maltodextrin's effect on the physicochemical and structure properties of spray dried orange juice powders. *European Food Research and Technology*, 1-8.

Igual, M., Ramires, S., Mosquera, L. H., & Martínez-Navarrete, N. (2014). Optimization of spray drying conditions for lulo (Solanum quitoense L.) pulp. *Powder technology*, *256*, 233-238.

Jalanka, J., Major, G., Murray, K., Singh, G., Nowak, A., Kurtz, C., Silos-Santiago, I., Johnston, J. M., de Vos, W. M., & Spiller, R. (2019). The effect of psyllium husk on intestinal microbiota in constipated patients and healthy controls. *International journal of molecular sciences*, *20*(2), 433.

Jalanka, J., Major, G., Murray, K., Singh, G., Nowak, A., Kurtz, C., Silos-Santiago, I., Johnston, J. M., de Vos, W. M., & Spiller, R. (2019). The effect of psyllium husk on intestinal microbiota in constipated patients and healthy controls. *International journal of molecular sciences, 20*(2), 433.

886 Jane, M., McKay, J., & Pal, S. (2019). Effects of daily consumption of psyllium, oat bran
887 and polyGlycopleX on obesity-related disease risk factors: A critical review. *Nutrition*, *57*,
888 84-91.
889
890 Jane, M., McKay, J., & Pal, S. (2019). Effects of daily consumption of psyllium, oat bran
891 and polyGlycopleX on obesity-related disease risk factors: A critical review. *Nutrition, 57*,
892 84-91.
893
894 Kale, M. S., Yadav, M. P., & Hanah, K. A. (2016). Suppression of psyllium husk
895 suspension viscosity by addition of water soluble polysaccharides. *Journal of food*
896 *science*, *81*(10), E2476-E2483.
897
898 Kwinda, O., Onipe, O. O., & Jideani, A. I. (2018). The effect of oat bran and psyllium
899 husk fibre on oil reduction and some physicochemical properties of magwinya–a deep-
900 fried dough. *CyTA-Journal of Food*, *16*(1), 247-254.
901
902 Lan, G., Chen, H., Chen, S., & Tian, J. (2012). Chemical composition and
903 physicochemical properties of dietary fiber from Polygonatum odoratum as affected by
904 different processing methods. *Food Research International*, *49*(1), 406-410.
905
906 Li, H. L., Xu, W. N., Jia, F. F., Li, J. B., Song, S. X., & Nahmad, Y. (2020). Correlation
907 between surface charge and hydration on mineral surfaces in aqueous solutions: A
908 critical review. *International Journal of Minerals, Metallurgy and Materials, 27*(7), 857-
909 871.
910

911 Li, X., Mao, L., He, X., Ma, P., Gao, Y., & Yuan, F. (2018). Characterization of β-
912 lactoglobulin gels induced by high pressure processing. Innovative *Food Science &*
913 *Emerging Technologies, 47*, 335-345.
914
915 Liu, F., R. Li, L. Mao, & Y. Gao. (2018). Ethanol-induced composite hydrogel based on
916 propylene glycol alginate and zein: Formation, characterization and application. *Food*
917 *Chemistry 255*, 390-8. DOI: 10.1016/j.foodchem.2018.02.072
918
919 Ma, M. M., & Mu, T. H. (2016). Effects of extraction methods and particle size distribution
920 on the structural, physicochemical, and functional properties of dietary fibre from deoiled
921 cumin. *Food Chemistry*, *194*, 237-246.
922
923 Mahdavi, S. A., Jafari, S. M., Assadpour, E., & Ghorbani, M. (2016). Storage stability of
924 encapsulated barberry's anthocyanin and its application in jelly formulation. *Journal of*
925 *Food Engineering*, *181*, 59-66.
926
927 Mao, L., Lu, Y., Cui, M., Miao, S., & Gao, Y. (2020). Design of gel structures in water and
928 oil phases for improved delivery of bioactive food ingredients. *Critical Reviews in Food*
929 *Science and Nutrition, 60*(10), 1651-1666. DOI: 10.1080/10408398.2019.1587737
930
931 Moghbeli, S., Jafari, S. M., Maghsoudlou, Y., & Dehnad, D. (2020). A Taguchi approach
932 optimization of date powder production by spray drying with the aid of whey protein-
933 pectin complexes. *Powder Technology*, *359*, 85-93.
934
935 Navarro-González, I., García-Valverde, V., García-Alonso, J., & Periago, M. J. (2011).
936 Chemical profile, functional and antioxidant properties of tomato peel fibre. *Food*
937 *Research International*, *44*(5), 1528-1535.

938

939 Niknam, R., Ghanbarzadeh, B., Ayaseh, A., & Rezagholi, F. (2018). The effects of
940 Plantago major seed gum on steady and dynamic oscillatory shear rheology of sunflower
941 oil-in-water emulsions. *Journal of texture studies, 49*(5), 536-547.

942

943 Noguerol, A. T., Pagán, M. J., Gracía-Segovia, P., & Varela, P. (2021). Green or Clean?
944 Perception of clean label plant-based products by omnivorous, vegan, vegetarian and
945 flexitarian consumers. Submitted.

946

947 Patel, M. K., Tanna, B., Gupta, H., Mishra, A., & Jha, B. (2019). Physicochemical,
948 scavenging and anti-proliferative analyses of polysaccharides extracted from psyllium
949 (Plantago ovata Forssk) husk and seeds. *International journal of biological*
950 *macromolecules, 133*, 190-201.

951

952 Patel, M. K., Tanna, B., Mishra, A., & Jha, B. (2018). Physicochemical characterization,
953 antioxidant and anti-proliferative activities of a polysaccharide extracted from psyllium
954 (P. ovata) leaves. *International journal of biological macromolecules*, *118*, 976-987.

955

956 Raghavendra, S. N., Rastogi, N. K., Raghavarao, K. S. M. S., & Tharanathan, R. N.
957 (2004). Dietary fiber from coconut residue: effects of different treatments and particle
958 size on the hydration properties. *European Food Research and Technology*, *218*(6),
959 563-567.

960

961 Ren, Y., Linter, B. R., & Foster, T. J. (2020a). Cellulose fibrillation and interaction with
962 psyllium seed husk heteroxylan. *Food Hydrocolloids*, *104*, 105725.

963

964 Ren, Y., Yakubov, G. E., Linter, B. R., MacNaughtan, W., & Foster, T. J. (2020b).
965 Temperature fractionation, physicochemical and rheological analysis of psyllium seed
966 husk heteroxylan. *Food Hydrocolloids*, *104*, 105737.
967
968 Ribes, S., Estarriaga, R., Grau, R., & Talens, P. (2021). Physical, sensory and simulated
969 mastication properties of texture-modified Spanish sauce using different texturing
970 agents. *Food & Function.*
971
972 Ribes, S., Peña, N., Fuentes, A., Talens, P., & Barat, J. M. (2021). Chia (Salvia hispanica
973 L.) seed mucilage as a fat replacer in yogurts: Effect on their nutritional, technological,
974 and sensory properties. *Journal of Dairy Science, 104*(3), 2822-2833.
975
976 Rosell, C. M., Santos, E., & Collar, C. (2009). Physico-chemical properties of commercial
977 fibres from different sources: A comparative approach. *Food Research*
978 *International*, *42*(1), 176-184.
979
980 Rousseau, S., Kyomugasho, C., Celus, M., Hendrickx, M. E., & Grauwet, T. (2020).
981 Barriers impairing mineral bioaccessibility and bioavailability in plant-based foods and
982 the perspectives for food processing. *Critical Reviews in Food Science and Nutrition,*
983 *60*(5), 826-843.
984
985 Sánchez-Moreno, C., Plaza, L., De Ancos, B., & Cano, M, P. (2003). Quantitative
986 bioactive compounds assessment and their relative contribution to the antioxidant
987 capacity of commercial orange juices. *Journal of the Science of Food and Agriculture*,
988 *83*, 430-439.
989

990 Selvendran, R.R., & Ryden, P. (1990). *Methods in plant biochemistry*, vol. 2 (pp.549)
991 London: Academic Press.
992
993 Shapovalov, V. M. (2017). On the applicability of the Ostwald–de Waele model in solving
994 applied problems. *Journal of Engineering Physics and Thermophysics, 90*(5), 1213-
995 1218.
996
997 Su, D., Zhu, X., Adhikari, B., Li, D., & Wang, L. (2020). Effect of high-pressure
998 homogenization on the rheology, microstructure and fractal dimension of citrus fiber-oil
999 dispersions. *Journal of Food Engineering, 277*, 109899.
1000
1001 Talens, P., Martinez-Navarrete, N., Fito, P., & Chiralt, A. (2002). Changes in optical and
1002 mechanical properties during osmodehydrofreezing of kiwi fruit. *Innovative Food Science*
1003 *& Emerging Technologies, 3*(2), 191-199.
1004
1005 Tejada-Ortigoza, V., Garcia-Amezquita, L. E., Serna-Saldívar, S. O., & Welti-Chanes, J.
1006 (2016). Advances in the functional characterization and extraction processes of dietary
1007 fiber. *Food Engineering Reviews*, *8*(3), 251-271.
1008
1009 Tomás-Barberán, F.A., Gil, M.I., Cremin, P., Waterhouse, A.L., Hess- Pierce, B., &
1010 Kader, A.A. (2001). HPLC-DAD-ESIMS Analysis of phenolic compounds in nectarines,
1011 peaches, and plums. *Journal of Agricultural and Food Chemistry*, *49*, 4748-4760.
1012
1013 Wang, Y., Sun, P., Li, H., Adhikari, B. P., & Li, D. (2018). Rheological behavior of tomato
1014 fiber suspensions produced by high shear and high pressure homogenization and their
1015 application in tomato products. *International journal of analytical chemistry*.
1016

1017 Yin, J. Y., Nie, S. P., Li, J., Li, C., Cui, S. W., & Xie, M. Y. (2012). Mechanism of
1018 Interactions between Calcium and Viscous Polysaccharide from the Seeds of Plantago
1019 asiatica L. *Journal of agricultural and food chemistry*, *60*(32), 7981-7987.
1020
1021 Yu, L. L., Perret, J., Parker, T., & Allen, K. G. D. (2003). Enzymatic modification to
1022 improve the water-absorbing and gelling properties of psyllium. *Food Chemistry, 82*,
1023 243–248.
1024
1025 Zhang, J., Wen, C., Zhang, H., & Duan, Y. (2019). Review of isolation, structural
1026 properties, chain conformation, and bioactivities of psyllium polysaccharides.
1027 *International journal of biological macromolecules, 139*, 409-420.
1028
1029 Zhu, K., Huang, S., Peng, W., Qian, H., & Zhou, H. (2010). Effect of ultrafine grinding on
1030 hydration and antioxidant properties of wheat bran dietary fibre. *Food Research*
1031 *International*, *43*(4), 943-948.
1032
1033 Ziemichód, A., Wójcik, M., & Różyło, R. (2019). Seeds of Plantago psyllium and Plantago
1034 ovata: Mineral composition, grinding, and use for gluten-free bread as substitutes for
1035 hydrocolloids. *Journal of food process engineering, 42*(1), e12931.

Figure Caption

Fig. 1. Image of *Psyllium* samples used in this study.

Fig. 2. Volume particle size distributions (representative curves) of fibre samples.

Fig. 3. *Psyllium* colour gel images at concentration tested (1-7%). Images taken on white background.

Fig. 4. Apparent viscosity (η_{ap}) vs shear rate of *Psyllium* gels.

Supplementary Figures

Fig. S1. PH real graph obtained from plasma optical emission spectrometer for mineral determination.

Fig. S2. PP real graph obtained from plasma optical emission spectrometer for mineral determination.

Fig. S3. Original back extrusion graph of *Psyllium* gel samples.

Fig. S4. Original flow curves of *Psyllium* gel samples.

Fig. S5. Original TPA graphs of *Psyllium* gel samples.

PH: Plantago Husk, PP: Plantago Powder.

Fig. 1.

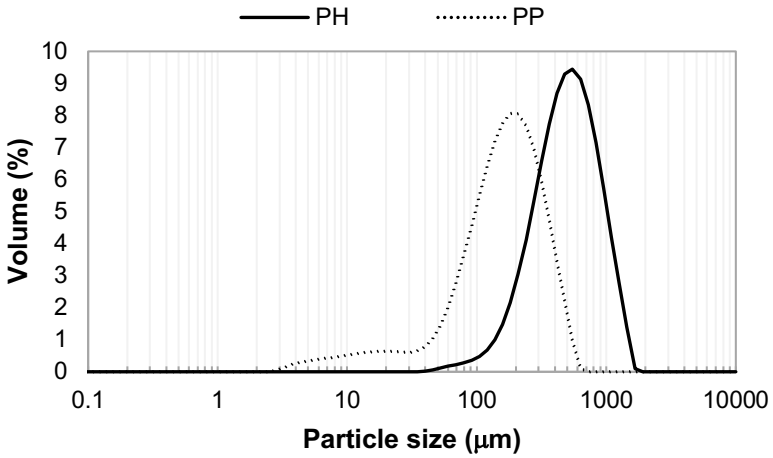

PH: Plantago Husk, PP: Plantago Powder.

Fig. 2.

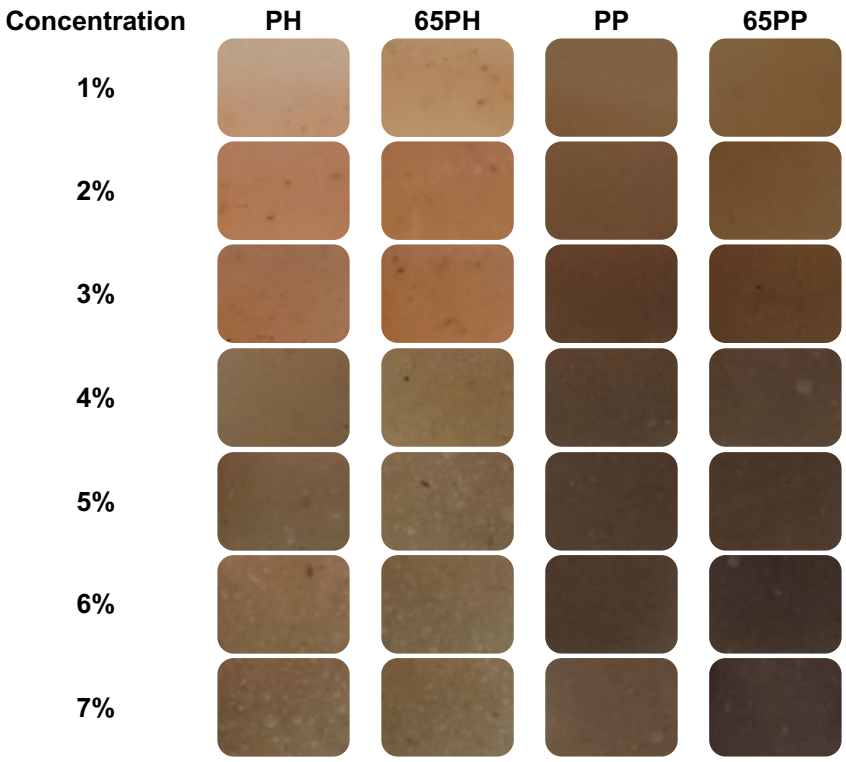

PH: Plantago Husk, PP: Plantago Powder

Fig. 3.

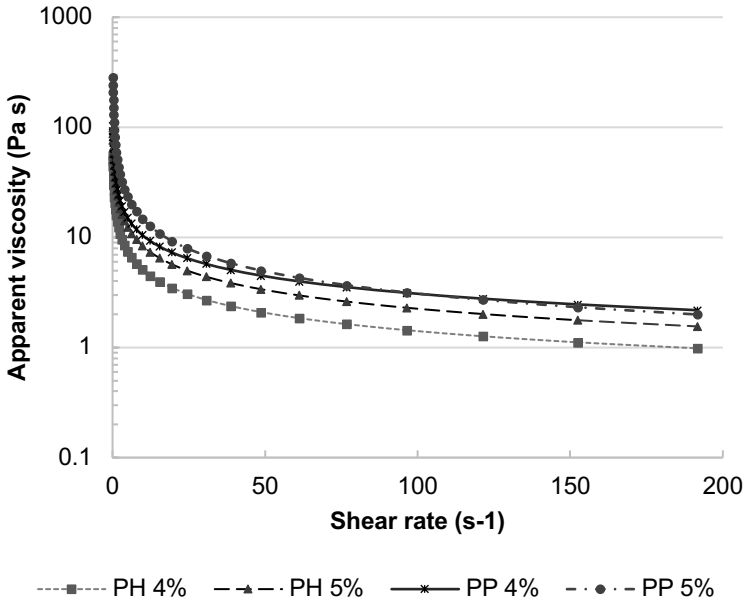

PH: Plantago Husk, PP: Plantago Powder.

Fig. 4.

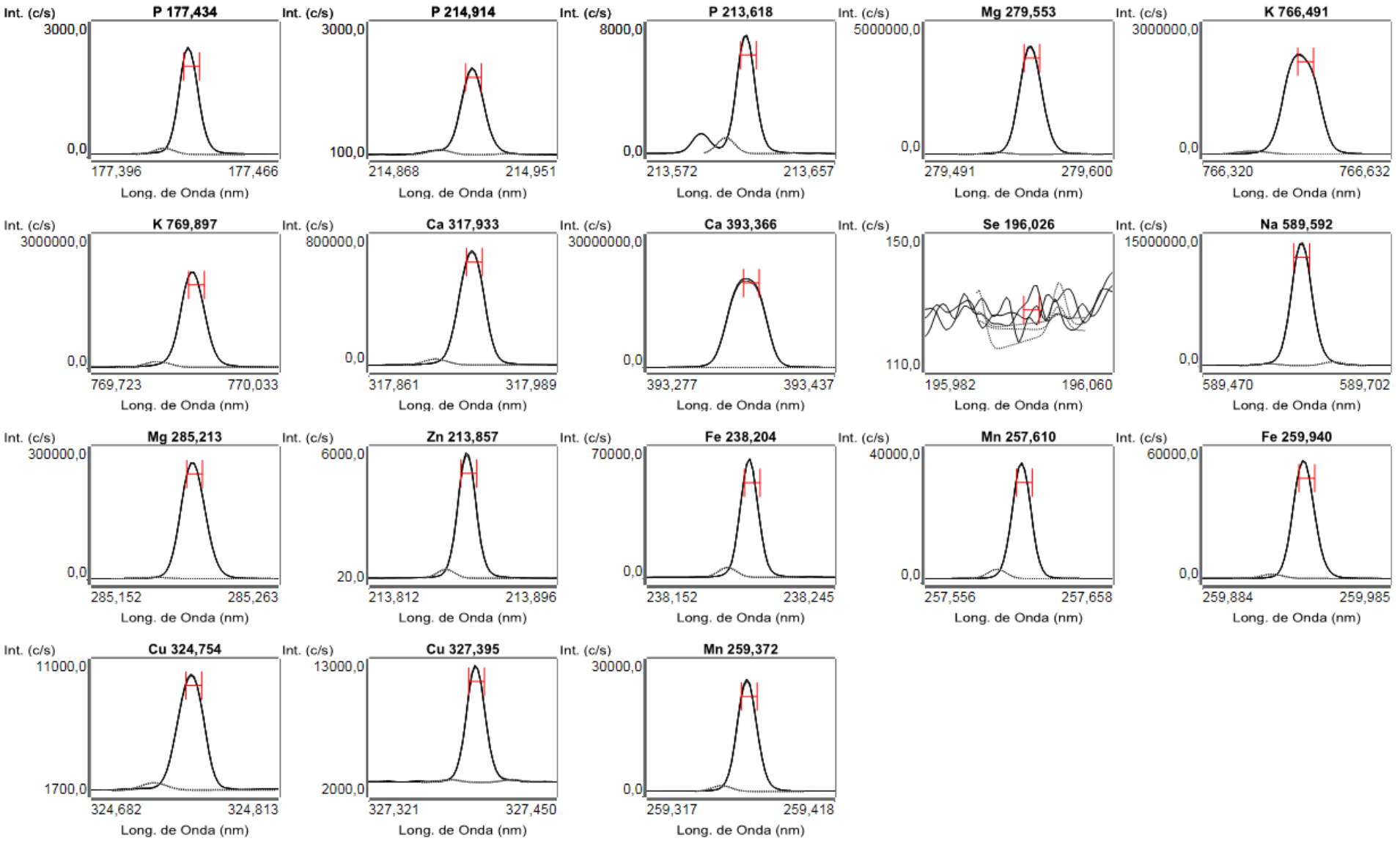
Int. (c/s)
P 177,434
3000,0
0,0
177,396
177,466
Long. de Onda (nm)
Int. (c/s)
P 214,914
3000,0
100,0
214,868
214,951
Long. de Onda (nm)
Int. (c/s)
P 213,618
8000,0
0,0
213,572
213,657
Long. de Onda (nm)
Int. (c/s)
Mg 279,553
5000000,0
0,0
279,491
279,600
Long. de Onda (nm)
Int. (c/s)
K 766,491
3000000,0
0,0
766,320
766,632
Long. de Onda (nm)
Int. (c/s)
K 769,897
3000000,0
0,0
769,723
770,033
Long. de Onda (nm)
Int. (c/s)
Ca 317,933
800000,0
0,0
317,861
317,989
Long. de Onda (nm)
Int. (c/s)
Ca 393,366
30000000,0
0,0
393,277
393,437
Long. de Onda (nm)
Int. (c/s)
Se 196,026
150,0
110,0
195,982
196,060
Long. de Onda (nm)
Int. (c/s)
Na 589,592
15000000,0
0,0
589,470
589,702
Long. de Onda (nm)
Int. (c/s)
Mg 285,213
300000,0
0,0
285,152
285,263
Long. de Onda (nm)
Int. (c/s)
Zn 213,857
6000,0
20,0
213,812
213,896
Long. de Onda (nm)
Int. (c/s)
Fe 238,204
70000,0
0,0
238,152
238,245
Long. de Onda (nm)
Int. (c/s)
Mn 257,610
40000,0
0,0
257,556
257,658
Long. de Onda (nm)
Int. (c/s)
Fe 259,940
60000,0
0,0
259,884
259,985
Long. de Onda (nm)
Int. (c/s)
Cu 324,754
11000,0
1700,0
324,682
324,813
Long. de Onda (nm)
Int. (c/s)
Cu 327,395
13000,0
2000,0
327,321
327,450
Long. de Onda (nm)
Int. (c/s)
Mn 259,372
30000,0
0,0
259,317
259,418
Long. de Onda (nm)

Fig. S1.

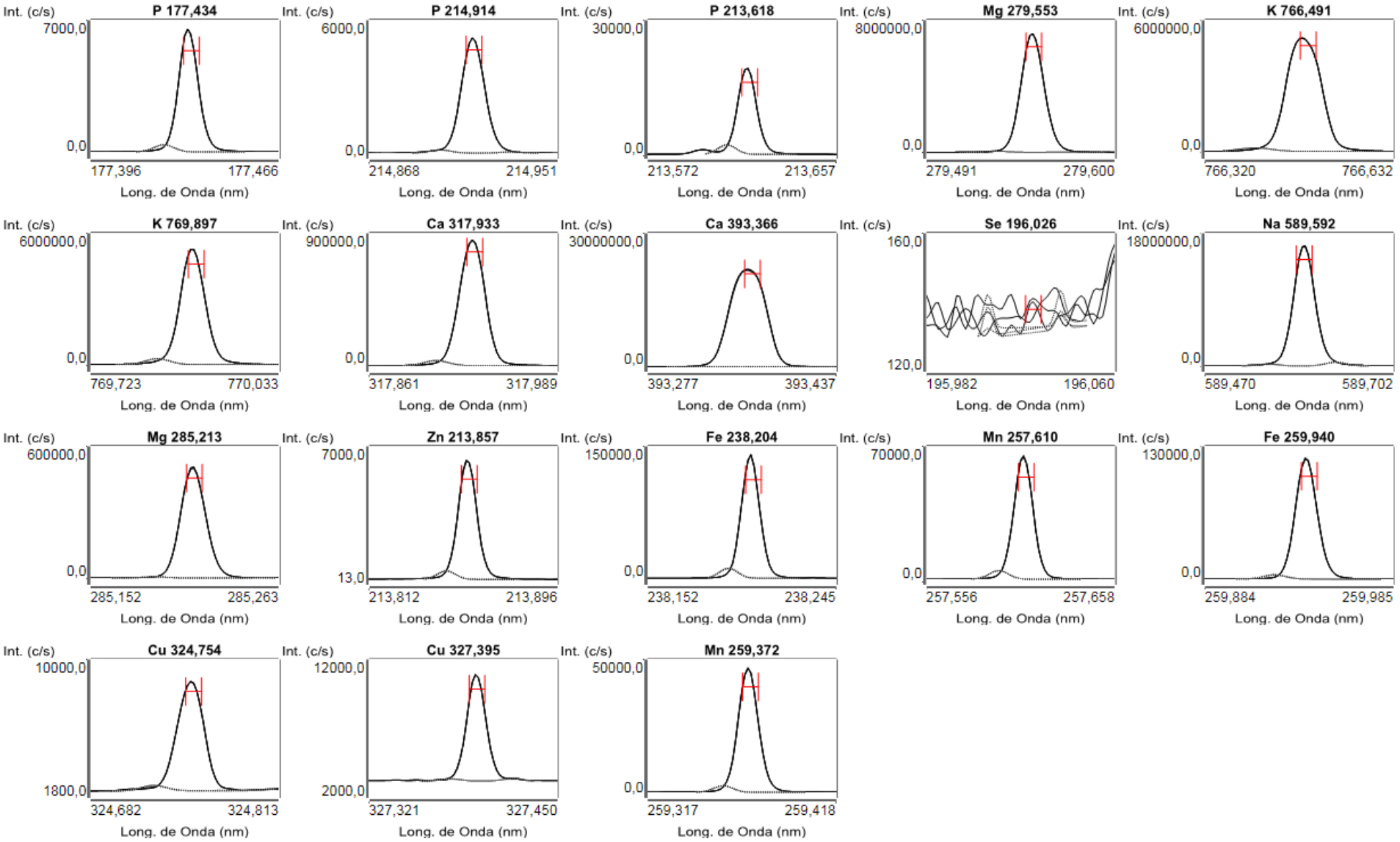
Int. (c/s)
P 177,434
7000,0
0,0
177,396
177,466
Long. de Onda (nm)
Int. (c/s)
P 214,914
6000,0
0,0
214,868
214,951
Long. de Onda (nm)
Int. (c/s)
P 213,618
30000,0
0,0
213,572
213,657
Long. de Onda (nm)
Int. (c/s)
Mg 279,553
8000000,0
0,0
279,491
279,600
Long. de Onda (nm)
Int. (c/s)
K 766,491
6000000,0
0,0
766,320
766,632
Long. de Onda (nm)
Int. (c/s)
K 769,897
6000000,0
0,0
769,723
770,033
Long. de Onda (nm)
Int. (c/s)
Ca 317,933
900000,0
0,0
317,861
317,989
Long. de Onda (nm)
Int. (c/s)
Ca 393,366
30000000,0
0,0
393,277
393,437
Long. de Onda (nm)
Int. (c/s)
Se 196,026
160,0
120,0
195,982
196,060
Long. de Onda (nm)
Int. (c/s)
Na 589,592
18000000,0
0,0
589,470
589,702
Long. de Onda (nm)
Int. (c/s)
Mg 285,213
600000,0
0,0
285,152
285,263
Long. de Onda (nm)
Int. (c/s)
Zn 213,857
7000,0
13,0
213,812
213,896
Long. de Onda (nm)
Int. (c/s)
Fe 238,204
150000,0
0,0
238,152
238,245
Long. de Onda (nm)
Int. (c/s)
Mn 257,610
70000,0
0,0
257,556
257,658
Long. de Onda (nm)
Int. (c/s)
Fe 259,940
130000,0
0,0
259,884
259,985
Long. de Onda (nm)
Int. (c/s)
Cu 324,754
10000,0
1800,0
324,682
324,813
Long. de Onda (nm)
Int. (c/s)
Cu 327,395
12000,0
2000,0
327,321
327,450
Long. de Onda (nm)
Int. (c/s)
Mn 259,372
50000,0
0,0
259,317
259,418
Long. de Onda (nm)

Fig. S2.

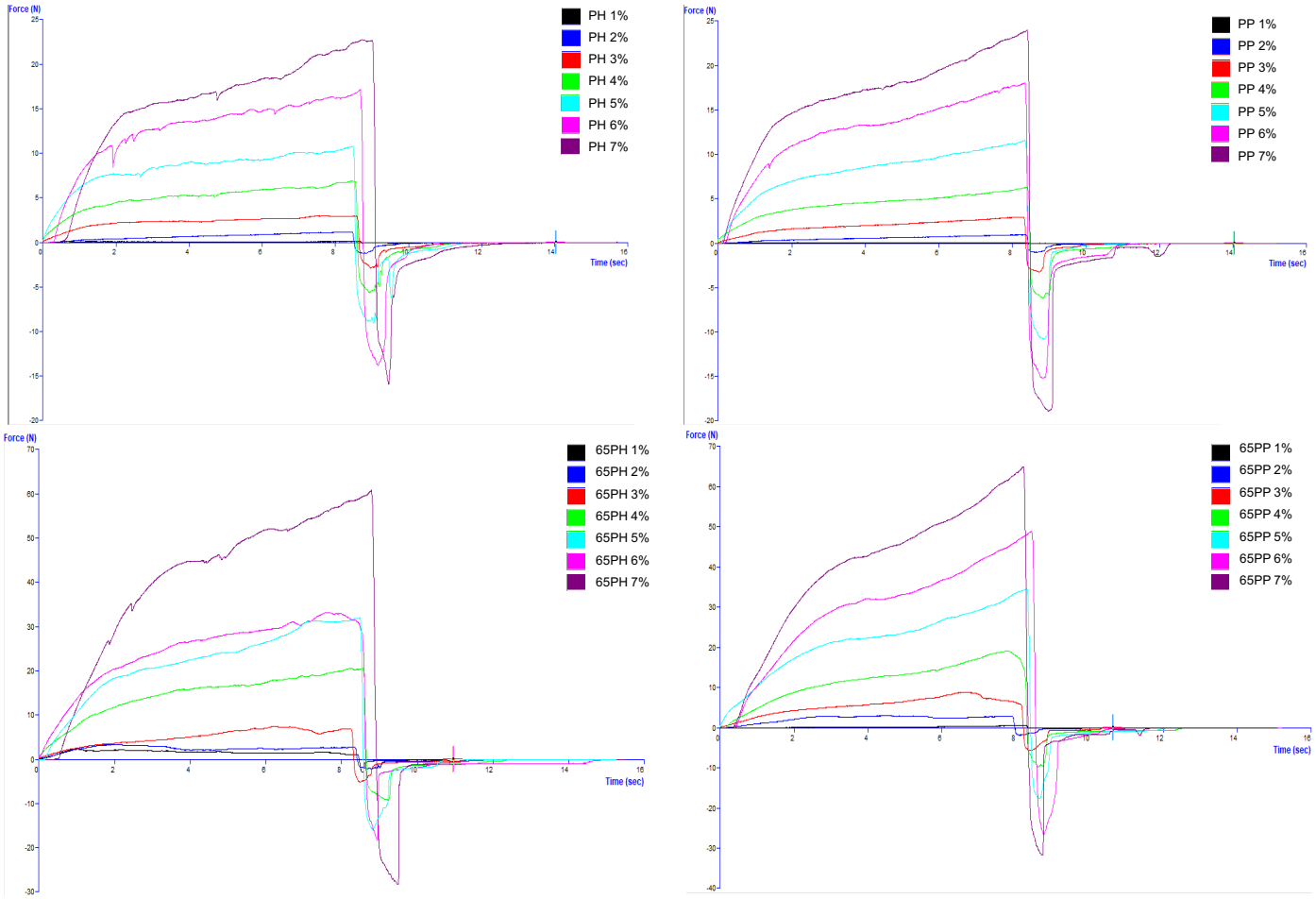
Force (N)
Time (sec)
PH 1%
PH 2%
PH 3%
PH 4%
PH 5%
PH 6%
PH 7%
PP 1%
PP 2%
PP 3%
PP 4%
PP 5%
PP 6%
PP 7%
65PH 1%
65PH 2%
65PH 3%
65PH 4%
65PH 5%
65PH 6%
65PH 7%
65PP 1%
65PP 2%
65PP 3%
65PP 4%
65PP 5%
65PP 6%
65PP 7%

Fig. S3.

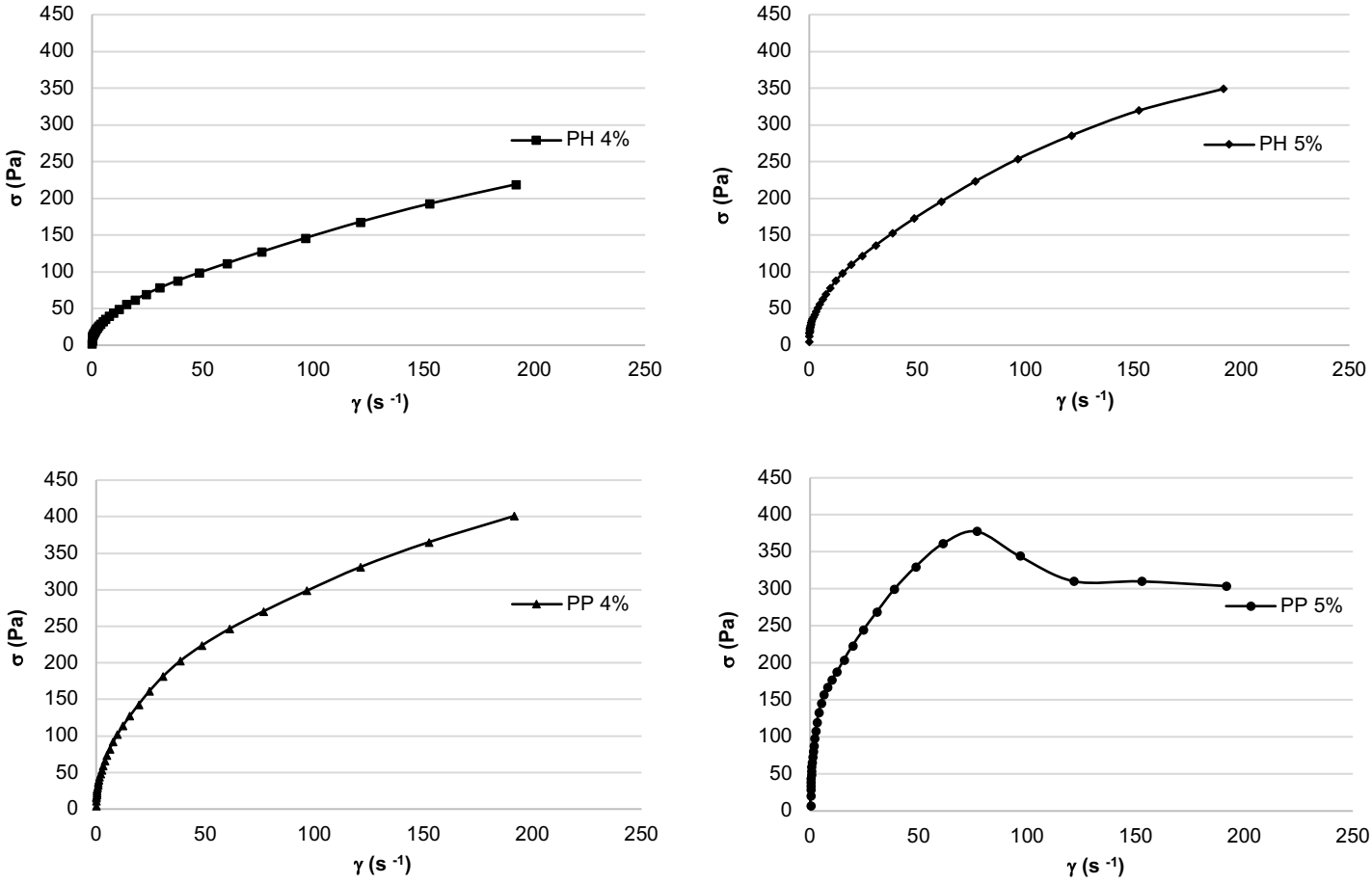

Fig. S4.

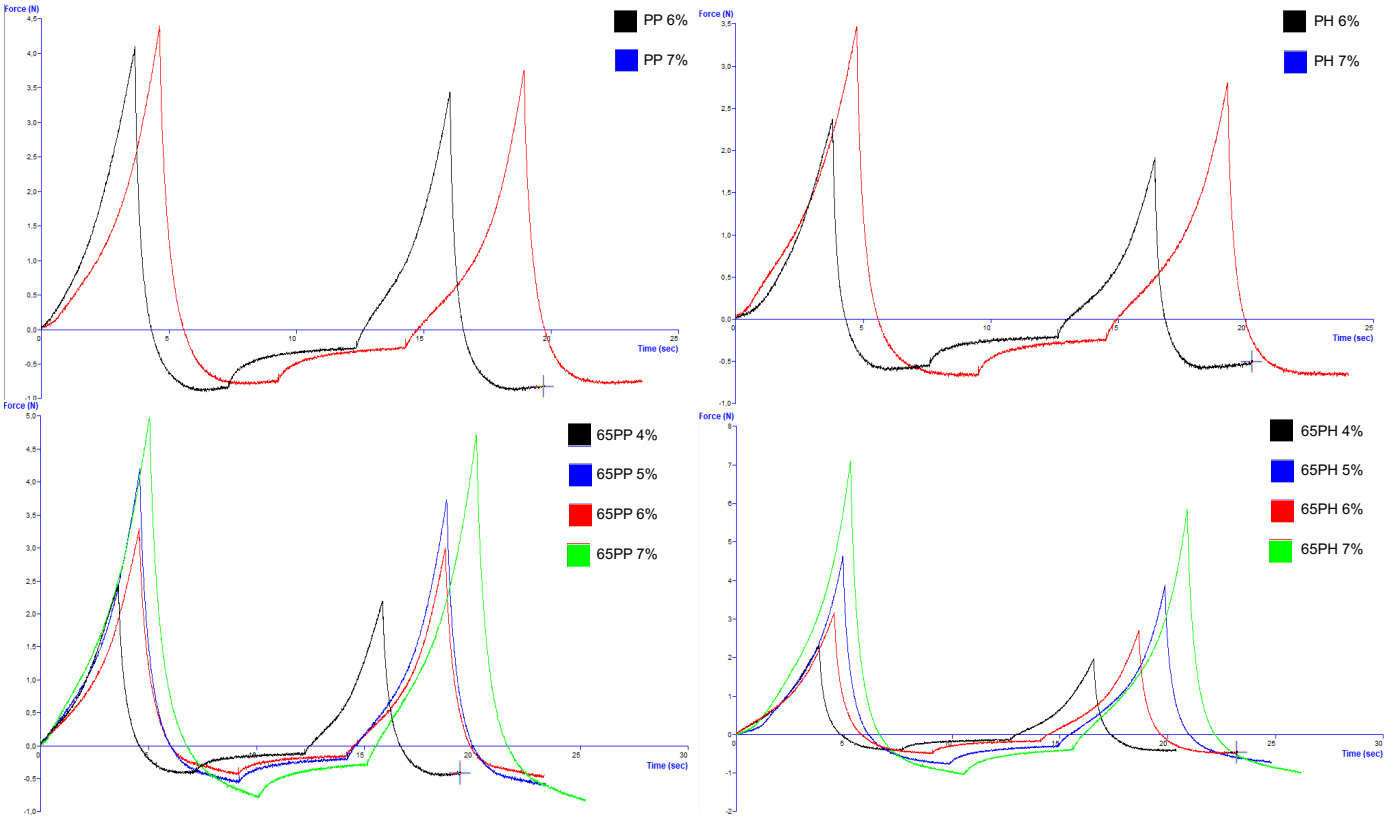
Force (N)
Time (sec)
PP 6%
PP 7%
PH 6%
PH 7%
65PP 4%
65PP 5%
65PP 6%
65PP 7%
65PH 4%
65PH 5%
65PH 6%
65PH 7%

Fig. S5.

Table 1. Name, ingredients and proximate sample composition. Data provided by suppliers.

	Samples	
	PH	**PP**
Name	Plantago Husk	Plantago Powder
Ingredients	*Psyllium* Husk 95%	*Plantago ovata* seeds
Protein	2.5	6.55
Lipids	0.5	1.8
Carbohydrates	4	8.53
TDF	78	70.5
IDF	77.1	28.4
SDF	0.9	42.1

TDF (Total dietary fibre); IDF (Insoluble dietary fibre); SDF (Soluble dietary fibre).

Table 2. Physicochemical and hydration properties of Plantago husk and Plantago powder.

	Samples	
	PH	**PP**
D[4,3] (μm)	597 (28)[a]	198 (4)[b]
d(0.1) (μm)	241 (20)[a]	48.2 (1.5)[b]
d(0.5) (μm)	535 (30)[a]	176 (2)[b]
d(0.9) (μm)	1051 (35)[a]	378 (8)[b]
a_w	0.324 (0.002)[a]	0.313 (0.005)[b]
x_w (g_{water}/100 g_{sample})	5.97 (0.14)[a]	5.1 (0.1)[b]
pH (dispersions 10% w/v)	5.93 (0.02)[b]	6.14 (0.03)[a]
Hg (g_{water}/100 $g_{dry\ solid}$)	34.8 (0.2)[a]	28.4 (0.2)[b]
ρ_b (g/L)	354 (7)[b]	472 (15)[a]
ε	76.9 (0.7)[a]	69 (1)[b]
WHC (g_{water}/$g_{dry\ sample}$)	27 (2)[a]	16.5 (1.9)[b]
WRC (g_{water}/$g_{dry\ sample}$)	25.8 (0.7)[a]	8.1 (1.3)[b]
SWC (mL_{water}/g_{sample})	11.7 (0.7)[a]	10.0 (0.9)[b]
WSI (%)	9.6 (0.5)[b]	37 (2)[a]
FAC (g_{oil}/g_{sample})	2.03 (0.06)[a]	1.01 (0.05)[b]

Mean values (and standard deviations).
The same letter in superscript in the line indicates the homogeneous groups established by ANOVA ($p < 0.05$).
PH: Plantago Husk, PP: Plantago Powder, D[4,3]: volume mean diameter, d(0.1), d(0.5), and d(0.9): standard percentiles, a_w: water activity, x_w: water content, Hg: hygroscopicity, ρ_b: bulk density, ε: porosity, WHC: water holding capacity, WRC: water retention capacity, SWC: swelling capacity, WSI: solubility, FAC: fat adsorption capacity.

Table 3. Total phenols (TP) (mg GAE/100 g sample), antioxidant capacity (AC) (mg TE/ 100 g sample), ash (%), total mineral content (mg/100 g sample) and individual mineral content (mg/100 g sample).

	Samples	
	PH	**PP**
Ash	2.104 (0.107)[b]	3.1 (0.2)[a]
Total mineral content	473 (19)[b]	792 (17)[a]
P	45 (6)[b]	123 (10)[a]
K	77.2 (1.3)[b]	200 (8)[a]
Ca	165 (6)[b]	204.2 (1.8)[a]
Se	0.06 (0.02)[a]	0.07 (0.03)[a]
Na	156 (6)[b]	193 (9)[a]
Mg	20 (5)[b]	50 (5)[a]
Zn	0.81 (0.06)[a]	1.1 (0.5)[a]
Fe	8 (2)[b]	21 (2)[a]
Cu	0.8 (0.2)[a]	0.49 (0.18)[a]
Mn	0.063 (0.005)[b]	0.74 (0.15)[a]
TP	55 (15)[b]	200 (9)[a]
AC	52 (7)[b]	126 (18)[a]

Mean values (and standard deviations).
The same letter in superscript in the line indicates the homogeneous groups established by the ANOVA ($p < 0.05$). PH: Plantago Husk, PP: Plantago Powder.

Table 4. Pearson correlation coefficients among hydration properties and physicochemical parameters and mineral content.

	SWC (mL_{water}/g_{sample})	WHC ($g_{water}/g_{drysample}$)	WSI (%)	WRC ($g_{water}/g_{drysample}$)	FAC (g_{oil}/g_{sample})
D[4,3] (μm)	0.8654*	0.9590*	-0.9936*	0.9900*	0.9925*
d(0.1) (μm)	0.8774*	0.9630*	-0.9909*	0.9857*	0.9882*
d(0.5) (μm)	0.8711*	0.9605*	-0.9926*	0.9884*	0.9909*
d(0.9) (μm)	0.8568*	0.9565*	-0.9946*	0.9923*	0.9947*
x_w ($g_{water}/100g_{sample}$)	0.7456	0.8698*	-0.9772*	0.9729*	0.9866*
a_w	0.7233	0.8912*	-0.8313*	0.9084*	0.8774*
Hg ($g_{water}/100g_{drysolid}$)	0.8281*	0.9604*	-0.9905*	0.9967*	0.9949*
pH	-0.8647*	0.9303*	0.9949*	-0.9633*	-0.9732*
ρ_b (g/L)	-0.7913	-0.9420*	0.9761*	-0.9957*	-0.9971*
ε	0.7668	0.9234*	-0.9845*	0.9843*	0.9894*
Total mineral ($mg/100g_{sample}$)	-0.8364*	-0.9496*	0.9960*	-0.9860*	-0.9883*
P ($mg/100g_{sample}$)	-0.7994	-0.9094*	0.9929*	-0.9729*	-0.9811*
K ($mg/100g_{sample}$)	-0.8722*	-0.9573*	0.9944*	-0.9898*	-0.9883*
Ca ($mg/100g_{sample}$)	-0.8593*	-0.9758*	0.9783*	-0.9729*	-0.9702*
Se ($mg/100g_{sample}$)	-0.2798	-0.4119	0.2273	-0.3423	-0.3258
Na ($mg/100g_{sample}$)	-0.7515	-0.9307*	0.9332*	-0.9401*	-0.9435*
Mg ($mg/100g_{sample}$)	-0.7578	-0.8848*	0.9727*	-0.9478*	-0.9548*
Zn ($mg/100g_{sample}$)	-0.5249	-0.6036	0.3601	-0.4710	-0.4036
Fe ($mg/100g_{sample}$)	-0.7968	-0.9088*	0.9794*	-0.9518*	-0.9572*
Cu ($mg/100g_{sample}$)	0.4314	0.5450	-0.6276	0.6515	0.6889
Mn ($mg/100g_{sample}$)	-0.8047	-0.8805*	0.9862*	-0.9472*	-0.9646*

*Correlation is significant at the 0.05 level

Volume mean diameter D[4,3], standard percentiles d(0.1), d(0.5) and d(0.9), water activity (a_w), water content (x_w), pH, hygroscopicity (Hg), bulk density (ρ_b), and porosity (ε); SWC: swelling capacity; WHC: water-holding capacity; WRC: water retention capacity; FAC: fat absorption.

Table 5. Results of x_w (g/g sample), the pH and colour parameters (L*, a* and b*) of the formulated *Psyllium* gels.

Samples	C	x_w	pH	L*	a*	b*
PH	1	0.9906 (0.0007)^{aA}	6.88 (0.06)^{aB}	6.5 (0.9)^{lG}	0.60 (0.04)^{deBC}	1.4 (0.4)^{hEF}
	2	0.9790 (0.0005)^{bC}	6.586 (0.109)^{cC}	11.4 (0.4)^{ijD}	1.64 (0.15)^{aA}	3.6 (0.3)^{dA}
	3	0.9697 (0.0009)^{dD}	6.39 (0.03)^{eD}	8.8 (0.7)^{kF}	0.72 (0.12)^{eCD}	0.83 (0.17)^{hF}
	4	0.9648 (0.0004)^{eE}	6.28 (0.08)^{fEF}	11.9 (0.9)^{iD}	0.77 (0.09)^{deBC}	1.1 (0.3)^{hEF}
	5	0.9522 (0.0009)^{fGH}	6.14 (0.02)^{ghH}	13.8 (1.3)^{hC}	0.96 (0.13)^{cdBC}	2.1 (0.5)^{gCD}
	6	0.9458 (0.0005)^{gI}	6.10 (0.02)^{hH}	26.1 (0.8)^{bA}	1.16 (0.07)^{cB}	3.2 (0.5)^{deAB}
	7	0.9412 (0.0003)^{hJ}	6.0 (0.3)^{iI}	25.1 (0.7)^{cA}	1.2 (0.4)^{cB}	2.8 (0.3)^{efB}
65PH	1	0.9879 (0.0018)^{yB}	7.01 (0.03)^{zA}	7 (2)^{sG}	0.49 (0.09)^{vE}	1.0 (0.2)^{vEF}
	2	0.9792 (0.0013)^{xC}	6.57 (0.12)^{xC}	9.92 (1.04)^{tEF}	0.516 (0.115)^{vDE}	0.8 (0.4)^{vEF}
	3	0.9689 (0.0006)^{wD}	6.32 (0.02)^{vE}	8.9 (0.7)^{utF}	0.42 (0.04)^{vE}	-0.24 (0.14)^{uG}
	4	0.96026 (0.00116)^{vF}	6.27 (0.04)^{utF}	10.8 (0.9)^{uDE}	0.78 (0.07)^{wBC}	1.3 (0.4)^{vEF}
	5	0.95384 (0.00115)^{uG}	6.188 (0.008)^{sG}	21.3 (0.7)^{xB}	0.82 (0.14)^{xwBC}	1.4 (0.6)^{vEF}
	6	0.95161 (0.00015)^{uH}	6.11 (0.03)^{qH}	22.5 (1.4)^{yxB}	0.87 (0.16)^{xwBC}	1.5 (0.5)^{wvDE}
	7	0.945 (0.002)^{tsI}	6.0 (0.3)^{pI}	21.5 (1.7)^{xB}	0.83 (0.15)^{xwBC}	2.1 (0.5)^{xwC}
PP	1	0.9898 (0.0012)^{aA}	6.71 (0.07)^{bA}	10.9 (0.8)^{jI}	0.45 (0.15)^{fFG}	1.2 (0.6)^{hG}
	2	0.9803 (0.0003)^{bB}	6.564 (0.009)^{cC}	15.0 (0.3)^{gH}	0.64 (0.09)^{efEF}	2.4 (0.4)^{fgEF}
	3	0.9734 (0.0004)^{cC}	6.51 (0.05)^{dD}	16.8 (0.3)^{fG}	1.03 (0.05)^{cC}	3.60 (0.13)^{dC}
	4	0.9644 (0.0002)^{eE}	6.40 (0.03)^{eE}	19.25 (0.13)^{eE}	1.40 (0.06)^{bB}	5.32 (0.19)^{cB}
	5	0.9547 (0.0002)^{fF}	6.3 (0.4)^{fFG}	21.5 (0.2)^{dD}	1.7600 (0.1114)^{aA}	6.6 (0.2)^{bA}
	6	0.9438 (0.0003)^{ghG}	6.16 (0.02)^{gI}	20.9 (0.4)^{dD}	1.76 (0.08)^{aA}	6.5 (0.2)^{bA}
	7	0.935 (0.007)^{iH}	6.2 (0.7)^{gI}	27.1 (0.6)^{aA}	1.6 (0.2)^{abAB}	7.1 (0.8)^{aA}
65PP	1	0.99060 (0.00013)^{zA}	6.64 (0.09)^{yB}	10.1 (0.9)^{utJ}	0.10 (0.05)^{uH}	-0.98 (0.16)^{tH}
	2	0.9794 (0.0005)^{xB}	6.404 (0.013)^{wE}	14.2 (0.8)^{vH}	0.33 (0.08)^{vG}	0.89 (0.08)^{vG}
	3	0.969 (0.003)^{wD}	6.29 (0.03)^{vuF}	16.7 (0.7)^{wG}	0.78 (0.07)^{wDE}	2.9 (0.5)^{zyDE}
	4	0.9620 (0.0003)^{vE}	6.244 (0.009)^{tG}	17.8 (0.3)^{wF}	1.02 (0.05)^{xC}	3.42 (0.15)^{zCD}
	5	0.9533 (0.0006)^{uF}	6.2 (0.4)^{sH}	26.1 (0.2)^{zB}	1.0 (0.2)^{xwCD}	2.3 (0.4)^{yxF}
	6	0.9453 (0.0008)^{tG}	6.148 (0.015)^{rI}	23.06 (1.08)^{yC}	1.5 (0.2)^{yB}	2.8 (0.8)^{zyDEF}
	7	0.9426 (0.0003)^{sG}	6.1 (0.7)^{qJ}	25.6 (0.6)^{zB}	1.7 (0.4)^{zA}	2.660 (1.114)^{yxEF}

Mean values (and standard deviations).

For the samples under the same conditions, the letter in superscript in the column indicates the homogeneous groups established by the ANOVA ($p < 0.05$) ($^{a–i}$ for unheated, and $^{z–q}$ heated samples). To compare the same sample to the temperature effect, the same capital letter in superscript in the column indicates the homogeneous groups established by the ANOVA ($p < 0.05$). C: Concentration (%); 65 indicates the samples heated at 65 ºC, 20 min; PH: Plantago Husk; PP: Plantago Powder.

Table 6. Back extrusion parameters of the formulated *Psyllium* gels.

Samples	C	Consistency (N s)	Firmness (N)	Viscosity (N s)	Cohesiveness (N)
PH	1	1.24 (0.08)^{gJ}	0.22 (0.02)^{gI}	0.08 (0.02)^{hG}	0.171 (0.012)^{iI}
	2	7 (3)^{fgIJ}	1.4 (0.5)^{fgI}	1.00 (0.02)^{ghFG}	1.3 (0.3)^{hHI}
	3	23 (8)^{eHI}	3.8 (1.4)^{eHI}	2.6 (0.7)^{fE}	3.3 (0.9)^{gG}
	4	43 (2)^{dGH}	6.8 (0.3)^{dGH}	4.64 (0.15)^{eD}	5.677 (0.109)^{fF}
	5	72 (5)^{cF}	11.7 (0.9)^{cF}	7.7 (0.7)^{cdC}	9.3 (0.4)^{eE}
	6	105 (6)^{bE}	16.9 (0.9)^{bE}	8.6 (0.5)^{cC}	13.2 (0.4)^{cD}
	7	142 (14)^{aD}	23.8 (1.7)^{aD}	10.1 (0.6)^{bB}	16.5 (0.8)^{bC}
65PH	1	8 (2)^{uIJ}	1.6 (0.5)^{rI}	0.62 (0.15)^{tFG}	1.5 (0.7)^{sGHI}
	2	24 (2)^{uHI}	3.6 (0.3)^{rHI}	2.0 (0.4)^{utEF}	2.6 (0.3)^{sGH}
	3	49 (14)^{vG}	9 (2)^{sFG}	4.2 (0.7)^{vD}	5.6 (1.2)^{tF}
	4	117 (15)^{wE}	21 (2)^{tDE}	8.2 (0.9)^{xwC}	9.6 (0.8)^{uE}
	5	168 (21)^{xC}	29 (3)^{uC}	10 (2)^{xB}	14.7 (1.7)^{vCD}
	6	234 (33)^{yB}	41 (8)^{wB}	13 (2)^{yA}	20 (3)^{xB}
	7	307 (42)^{zA}	53 (9)^{yA}	14 (3)^{zyA}	24 (4)^{yA}
PP	1	1.04 (0.02)^{gK}	0.16 (0.04)^{gJ}	0.056(0.003)^{hH}	0.148 (0.005)^{iH}
	2	5.5 (0.5)^{gJK}	1.049 (0.109)^{gIJ}	0.71 (0.05)^{hGH}	1.04 (0.05)^{hiGH}
	3	16 (3)^{efIJ}	2.8 (0.6)^{efHI}	2.16 (0.18)^{fgFG}	3.1 (0.3)^{gG}
	4	36 (8)^{dH}	6.1 (1.6)^{dG}	4.5 (0.6)^{eE}	6.14 (1.06)^{fF}
	5	68 (5)^{cF}	11.8 (0.8)^{cF}	6.992 (1.112)^{dD}	10.8 (0.4)^{dE}
	6	106 (7)^{bE}	18.22 (1.09)^{aE}	8.87 (1.18)^{bcCD}	14.0 (1.5)^{cD}
	7	145 (15)^{aD}	25 (3)^{bD}	13 (3)^{aB}	18.8 (1.9)^{aC}
65PP	1	2.68 (0.09)^{uJK}	0.57 (0.07)^{rJ}	0.176 (0.006)^{tGH}	0.23 (0.02)^{sH}
	2	23 (3)^{uHI}	3.8 (0.5)^{rH}	1.47 (0.09)^{tGH}	2.08 (0.09)^{sGH}
	3	52 (6)^{vG}	9.73 (1.04)^{sF}	4.0 (0.4)^{vuEF}	6.6 (0.6)^{tF}
	4	102 (7)^{wE}	19.8 (1.7)^{tE}	7.7 (0.7)^{wCD}	11.0 (0.7)^{uE}
	5	178 (9)^{xC}	34.362 (1.009)^{vC}	9.1 (1.4)^{xwC}	17.5 (0.7)^{wC}
	6	247 (7)^{yB}	47 (2)^{xB}	14.1 (1.4)^{zyAB}	24.71 (1.08)^{yB}
	7	298 (30)^{zA}	61 (4)^{zA}	15 (5)^{zB}	28 (5)^{zA}

Mean values (and standard deviations).

For the samples under the same conditions, the letter in superscript in the column indicates the homogeneous groups established by the ANOVA ($p < 0.05$) ($^{a–i}$ for unheated, and $^{z–r}$ heated samples). To compare the same sample to the temperature effect, the same capital letter in superscript in the column indicates the homogeneous groups established by the ANOVA ($p < 0.05$). C: Concentration (%); 65 indicates the samples heated at 65 ºC, 20 min; PH: Plantago Husk; PP: Plantago Powder.

Table 7. Flow curve parameters *k* (consistency index), *n* (flow index) and η_{ap} (shear viscosity at 50 s^{-1} shear stress) of the formulated *Psyllium* gels.

Ostwald-de Waele model					
Samples	**C (%)**	***k* (Pa s^n)**	***n***	**η_{ap} (Pa s)**	**R^2**
PH	4	21.5 (0.3)^c	0.468 (0.006)^a	2.7 (0.04)^b	0.99
	5	24 (3)^c	0.464 (0.016)^a	3.0 (0.2)^b	0.99
PP	4	42 (2)^b	0.404 (0.007)^b	4.10 (0.09)^a	0.99
	5	69.4 (0.5)^a	0.32 (0.05)^c	4.91 (1.02)^a	0.99

Mean values (and standard deviations).

The same letter in superscript in the line indicates the homogeneous groups established by the ANOVA ($p < 0.05$). C: concentration (%); PH: Plantago Husk; PP: Plantago Powder.

Table 8. TPA parameters of the formulated *Psyllium* gels.

Samples	C	Hardness	Adhesiveness	Springiness	Cohesiveness	Resilience	Chewability
PH	6	2.7 (0.4)^{bCD}	-3.2 (0.3)^{cC}	0.90 (0.03)^{aAB}	0.69 (0.02)^{bC}	0.12 (0.02)^{cD}	1.69 (0.19)^{cCD}
	7	3.2 (0.3)^{bC}	-3.89 (0.19)^{bB}	0.89 (0.02)^{aB}	0.72(0.03)^{bBC}	0.142 (0.016)^{bC}	2.0 (0.2)^{bC}
65PH	4	2.37 (0.14)^{wD}	-1.839 (0.117)^{vuE}	0.914 (0.008)^{zA}	0.708 (0.007)^{wC}	0.185 (0.018)^{vuB}	1.535 (0.104)^{vD}
	5	3.0 (0.3)^{xC}	-2.4 (0.3)^{wD}	0.91523 (0.01107)^{zA}	0.7337 (0.0104)^{wB}	0.206 (0.005)^{xwvAB}	2.0 (0.2)^{wC}
	6	4.7 (0.3)^{yB}	-4.0 (0.3)^{yB}	0.898 (0.013)^{zAB}	0.777 (0.008)^{yxA}	0.200 (0.009)^{wvAB}	3.3 (0.3)^{yB}
	7	6.2 (0.7)^{zA}	-4.9 (0.6)^{zA}	0.9021 (0.0103)^{zAB}	0.7678 (0.0115)^{xA}	0.217 (0.016)^{yxwA}	4.3 (0.6)^{zA}
PP	6	4.0 (0.4)^{aB}	-3.95 (0.14)^{bAB}	0.916 (0.013)^{aA}	0.760 (0.017)^{aD}	0.141 (0.012)^{bC}	2.8 (0.3)^{aBC}
	7	4.1 (0.5)^{aAB}	-4.31 (0.17)^{aA}	0.889(0.015)^{aB}	0.78 (0.03)^{aCD}	0.186 (0.009)^{aB}	2.9 (0.3)^{aBC}
65PP	4	2.3 (0.3)^{wD}	-1.99 (0.18)^{vD}	0.90 (0.02)^{zAB}	0.83(0.04)^{zAB}	0.19 (0.03)^{vuB}	1.70 (0.19)^{wvD}
	5	3.5 (0.2)^{xC}	-2.20 (0.09)^{wvuD}	0.909 (0.013)^{zAB}	0.793 (0.013)^{yxC}	0.242 (0.014)^{zyA}	2.51 (0.14)^{xC}
	6	4.3 (0.6)^{yAB}	-3.0 (0.6)^{xC}	0.902 (0.019)^{zAB}	0.80 (0.03)^{yBC}	0.250 (0.019)^{zA}	3.1 (0.4)^{yB}
	7	4.6 (0.4)^{yA}	-3.7 (0.5)^{yB}	0.9077 (0.0104)^{zAB}	0.833 (0.016)^{zA}	0.23 (0.02)^{zyxA}	3.5 (0.3)^{yA}

Mean values (and standard deviations).

For the samples under the same conditions, the same letter in superscript in the column indicates the homogeneous groups established by the ANOVA ($p < 0.05$) ($^{a–c}$ for unheated, and $^{z–u}$ heated samples). To compare the same sample to the temperature effect, the same capital letter in superscript in the column indicates the homogeneous groups established by the ANOVA ($p < 0.05$). C: Concentration (%); 65 indicates the samples heated at 65 ºC, 20 min; PH: Plantago Husk; PP: Plantago Powder.